1986

Analysis of track and wheel soil compaction

Philip Walter Gassman
Iowa State University

Analysis of track and wheel soil compaction

by

Philip Walter Gassman

A Thesis Submitted to the

Graduate Faculty in Partial Fulfillment of the

Requirements for the Degree of

MASTER OF SCIENCE

Major: Agricultural Engineering

Approved:

_____

In Charge of Major Work

_____

For the Major Department

_____

For the Graduate College

Iowa State University
Ames, Iowa

1986

TABLE OF CONTENTS

INTRODUCTION

Compaction of agricultural soils induced by heavy farm machinery has been a matter of increasing concern in recent years. An element of soil, when subjected to pressure from vehicle loading, will experience a decrease in volume. Thus, the soil density will increase, resulting in a reduction in pore space and an increase in the soil strength. Reduced pore space leads to restricted aeration and drainage of the soil, which are harmful for root growth. Also, the increased soil strength of a compacted soil impedes the growth of roots. Ultimately, these negative compaction effects are responsible for reduced crop yields and less profit for the farmer.

Of particular concern is the amount of compaction, occurring in the subsoil (below the tillage zone), that cannot be alleviated by normal tillage practices. Restricted root growth and reduced yields due to subsoil compaction have been verified by several researchers (Gaultney et al., 1982, Schuler and Lowery, 1984; Blake et al., 1976; Wittsell and Hobbs, 1965; Voorhees, 1977).

The need exists to study different types of vehicles and tractive devices to gain additional insight into the relationship between vehicle applied loads and soil compaction. There is some indication that track-type tractors (TTT) may compact soil less than wheel-type tractors (WTT). Several studies comparing TTTs and WTTs have produced evidence that less compaction occurs beneath TTTs (Reaves and Cooper, 1960; Soane, 1973; Taylor and Burt, 1975; Janzen et al., 1985). However, other studies found no compaction difference

between TTTs and WTTs (Brixius and Zoz, 1976; Burger et al., 1983).

The ability to predict soil compaction due to vehicle loading would be a major step in determining the degree and depth of compaction that could occur for a particular vehicle. A model that could simulate the loading from a TTT or WTT, and incorporate realistic characteristics of soil, would be a useful tool for predicting compaction.

The advent of powerful digital computers, coupled with the development of computational analysis techniques, provide the means to predict how soil will respond under loading. Numerical procedures allow the constitutive behavior of soil to be modeled, a requirement for accurate modeling of compaction.

One numerical procedure that can model the compaction of soil due to vehicle loading is the finite element method. The finite element method can handle nonlinear and layered properties of soil. Variations in loading can be simulated and resulting soil strains or compaction can be predicted.

Thus, the specific goals of this research are:

1. To develop a finite element model that can predict soil compaction beneath TTTs and WTTs.
2. To use the model to examine how variations of loading affect the depth of compaction.
3. To observe the model predictions of strain for layered and uniform soil conditions.

REVIEW OF LITERATURE

Boussinesq Theory

The majority of modeling work concerning vehicle induced soil compaction has concentrated on simulating compaction due to WTTs. This is because most of the tractors employed in present day agriculture are WTTs. Of the modeling methods used to predict soil compaction the most widely used have been analytical procedures based on Boussinesq theory.

Boussinesq theory assumes that the soil is a semi-infinite, homogeneous, isotropic, elastic medium (Wong, 1978). Using Boussinesq equations, the stress distribution in a soil can be determined for a point load acting at the surface. These stresses are independent of the modulus of elasticity and are simply functions of the load applied and the distance from the point of application of the load.

Soehne (1958) developed modified Boussinesq equations that simulated loading over the total tire-soil contact area instead of using just a point load. He also employed concentration factors that were intended to simulate conditions of a hard dry soil, a normal soil, and a wet soil. The hard dry soil was considered to be mostly elastic while the wet soil was considered to be very plastic.

Soehne (1958) used his modified Boussinesq equations to predict the stress distributions in a soil from simulated tire loads. He calculated the stress distributions for different size tires at their

rated loads, while assuming the same inflation pressure and the same tire-soil surface contact pressure for each tire. His findings indicated that the compaction close to the soil surface is mainly a function of the contact pressure of the tractive device while the compaction in the subsoil is a function of the total load. Other studies employing Boussinesq theory have yielded similar results (Blackwell and Soane, 1981; Carpenter and Fausey, 1983; Bowen et al., 1984).

Other research work indicates that the width of a tractive device influences the depth of compaction. Porterfield and Carpenter (1985) developed a potential compaction index based on Boussinesq theory, where the relative degree of compaction was calculated to be the product of the mean tire contact pressure and the tire contact width. While the results indicated that the total load was the major factor involved in subsoil compaction, it was determined that tire width also influences the depth of compaction. Alekseeva et al. (1972) comment that as the transverse dimension of a contact surface increases, for a given pressure, the depth of compaction will increase. Taylor (1985) indicates that long, narrow footprints reduce the amount of field area subjected to compactive forces along with improving tractive efficiency.

Taylor et al. (1980) conducted experiments to examine how well Boussinesq theory correlated with actual measurements. The tests were conducted with two types of soils and two different soil conditions. The pressure measurements were obtained in a soil bin

under two different size tires, that were loaded at their rated loads and had the same inflation pressure. They assumed that the surface contact pressures of the two tires were the same. The predictions of the Boussinesq equation compared reasonably well with the experimental results for soil conditions that were essentially homogeneous. However, when a hard layer was introduced into the soil at a depth of approximately 20 cm, The Boussinseq theory no longer held. The same discovery was made by Gameda et al. (1984), who found that the applicability of Boussinesq theory is more appropriate for homogeneous, nonlayered soils.

Bekker (1956) applied the Boussinesq theory to determine the stress isograms that result beneath the width of TTT track. The soil was considered to be a semi-infinite elastic medium. He found that at a depth equal to the width of the track, the vertical stress under the center of the loaded area is approximately fifty percent of the applied pressure, and at a depth twice the width of the track the vertical stress basically vanishes.

Finite Element Method

Perumpral et al. (1971) were the first to use the finite element method to study soil-vehicle interaction. They employed the finite element method to predict the stress distribution and soil deformation under a stationary and a moving tractor wheel. In their analysis of the stationary tractor wheel, it was assumed that the wheel-soil contact area, which is generally elliptical

in shape, was circular. This allowed the wheel-soil interaction to be modeled as a two-dimensional, axisymmetric case, where the loading was applied as a uniform pressure in the normal direction. Only one-half of the system was analyzed, because it was assumed that the loading was symmetrical about the vertical axis. The soil used in the stationary analysis was Ottawa sand, compacted close to its maximum density. It was assumed to be a nonlinear elastic, homogeneous, isotropic material. The stress-strain relationship input into the model was determined by triaxial tests.

Perumpral et al. (1971) analyzed the moving wheel as a plane-strain problem. This assumption required that the wheel width be considered infinite and that the radial and tangential stress distributions, determined in a previous experiment, remained constant with the wheel width. The moving wheel was modeled as a two-dimensional problem. Two different types of soil conditions were used. The first condition assumed that the modulus of elasticity was constant, while the second assumed that the modulus of elasticity increased linearly with depth. The soil was considered to be linearly elastic, homogeneous, and isotropic in both cases.

The results of the stationary wheel analysis by Perumpral et al. (1971) agreed favorably with elastic theory. However, the predicted results did not not agree well with experimental results. No experimental verification of the moving wheel problem was conducted.

Yong and Fattah (1976) used the finite element method for predicting continuous rigid wheel performance and subsoil response

behavior. The model simulated the process of soil loading and unloading upon application of the wheel load. A two-dimensional model was used in the study. The load boundary conditions were radial and tangential stresses, determined experimentally, applied along the length of the wheel-soil contact area. The soil constitutive properties were based on a nonlinear elastic relationship, determined from triaxial tests conducted on a uniform clay soil. The predicted rut depth, bow wave, velocity contours in the soil, and deformation energy contours predicted by the model agreed well with experimental results.

Yong et al. (1978) employed the finite element method to study the interaction of a moving wheel with a relatively stiff soil. The flexibility of a typical tire carcass was taken into account in this model. The wheel was idealized as a cylindrical body of infinite width, which again allowed the wheel-soil interaction to be analyzed as a two-dimensional plane strain problem. The contact area was assumed to be rectangular and the length of the wheel was modeled. Pressures were input at the wheel-soil interface in the form of a parabolic relationship to simulate peak pressures found from actual measurements of the tires used in the study.

The soil used by Yong et al. (1978) was a laboratory prepared mixture of fine silica sand, kaolinite clay (proportioned at thirty percent of the dry sand weight), and water. The soil was compacted in a soil bin to a uniform dry density of 1.88 Mg/m^3 at a moisture content of thirteen percent. Soil samples were taken from

the soil bin and tested in plane-strain triaxial compression tests. The constitutive soil properties used in the model were piece-wise, nonlinear elastic relationships, based on the triaxial tests. The predicted results of the study compared favorably with tests conducted with three different tires in a soil bin.

Oida (1984) used the finite element method to predict the time-dependent sinkage of a rigid wheel into a sandy loam soil. He used a two-dimensional model in which one-half of the wheel-soil plane was modeled. The load boundary condition was the axial load of the wheel. The load was applied along the length of the wheel. The constitutive nature of the soil was simulated by linear viscoelastic analysis. The predicted results of Oida's model for various combinations of loading and soil moisture content compared favorably with experimental measurements. No attempt was made to determine how much compaction occurred in the soil.

Pollock et al. (1984) used the finite element method to predict the amount of soil compaction from single and multiple wheel loading by a pneumatic tire. They assumed the tire-soil contact area to be circular and employed a two-dimensional, axisymmetric model to simulate the compaction process. The loading was symmetrical about the vertical axis, requiring only one-half of the system to be analyzed. The load boundary conditions were applied as normal pressures. A hyperbolic model was used to represent the soil stress-strain relationship. The soils used in the study were a sand and a clay, for which model parameters were known.

Pollock et al. (1984) used volumetric strain to model the degree of compaction. The results indicated that the point of maximum compaction may occur at some finite depth below the soil surface. This agrees with a laboratory study conducted by Chancellor et al. (1962). The results also indicated that with a decrease in loading pressure, a significant decrease in compaction occurred. The model results were not experimentally verified.

Turner (1984) used the finite element method to study the interaction of a TTT with soil. However, he was concerned with predicting the thrust-slip characteristics of track systems and did not consider soil compaction.

MATERIALS AND METHODS

Model Theory

The finite element method is a mathematical technique which has become a popular way of solving a wide variety of continuum mechanics problems. With this method, a given continuum is divided into a finite number of discrete elements which are connected together at nodal points. Constitutive equations, based on the governing partial differential equations, are written for each element. These constitutive equations are then assembled into a larger matrix equation which is solved by means of a computer. A more complete discussion of the finite element method can be readily found in any finite element textbook.

Finite element models employed in the past for studying vehicle-soil interaction have been fairly successful in predicting certain aspects of soil response due to vehicle loading. However, the soils incorporated in these models have usually been sand or clay, while very little modeling work has been done with agricultural soils. There was also no mention in the literature of comparing predicted results from a model with measured results in a field situation. Therefore, the model in this research was designed so that vehicle loads could be applied to an agricultural soil, with the predicted results compared to field measurements.

Past finite element modeling of vehicle-soil interaction has relied on several basic assumptions to simplify the problem. It is

necessary to modify some of these assumptions in order to model vehicle loading upon an agricultural soil.

Typically, the soil is considered to be a homogeneous and isotropic material. In reality, soil is a very complex material that varies in both space and time. Because soil is composed of granular materials of different sizes, liquids, and gases, it is very difficult to define.

One way of more closely simulating real soil is to include distinct layers with different properties in the model. While the layers are homogeneous and isotropic within themselves, the soil mass as a whole is not. Soehne (1958) points out that the modulus of elasticity for a soil is not constant but generally increases with depth. Therefore, layers of soil are included in the model to simulate this effect.

Another major assumption often made in finite element modeling of soil is that the soil is an elastic material. However, vehicle loading produces large stresses that permanently deform the soil. Thus, for this model the soil is considered to be an elastic-plastic material.

A third assumption made in some models is that the elliptical wheel-soil contact area can be approximated by an equivalent circular contact area, where the load is applied as a uniformly distributed pressure over the contact area. This allows the problem to be analyzed as an axisymmetric, two-dimensional problem instead of a three-dimensional problem. This assumption is reasonable for a tire

but not for a track. For this reason, a plane strain analysis was chosen for the model. This type of analysis assumes that the tractive device is very long and that the loading is uniform along the length. It is also assumed that no strain occurs in the direction of travel. While these may not be totally accurate, these assumptions allow the problem to be analyzed with a two-dimensional model and avoid the complexity and cost of a three-dimensional analysis.

The simulated vehicle loads for the model were applied as uniform, static pressures. These pressures were assumed to be equal to the contact pressure between the tractive device and the soil. For a TTT, the contact pressure was assumed to be equal to the nominal mean ground pressure, which is the load divided by the contact area of the tracks. For a WTT the contact pressure was assumed to be equal to the inflation pressure of the tire.

The contact pressure was applied along the width of the tractive device instead of along the length. The width is assumed to play a more important role in the compaction process than the length because any given vehicle will traverse the same amount of distance for a field operation, but the width of the track will vary.

A final consideration for the model is to include the bulk density of the soil. By including values of the bulk density prior to compaction, it is hoped that the model will predict accurate values of bulk density after the loads have been applied.

Development of Model

The finite element model was developed in ANSYS, a general purpose finite element program developed by Swanson Analysis Systems, Inc. (Desalvo, G. J. and J. A. Swanson, 1985). ANSYS is widely used throughout industry for structural analysis of mechanical systems and for solving other continuum mechanics problems. The program was chosen for this research because it can handle nonlinear material behavior and incorporate different material properties in the same model.

The mesh of rectangular elements used in the finite element model is shown in Figure 1. It represents a cross-section of soil in the x-y plane, 106.7 cm wide and 106.7 cm deep. The origin is at the upper left corner. The upper boundary is the positive x-axis while the left, vertical boundary is the negative y-axis. The vertical boundaries are constrained so that no movement can occur in the x-direction (denoted by the triangles in Figure 1). The lower horizontal boundary is constrained so that no movement can occur in the y-direction. The idealized system is represented by 144 nodes and 121 elements.

The boundary on the left side of the model represents the plane of symmetry beneath the center of a given tractive device. Because the loading and soil reaction can be assumed to be symmetrical about the center of the tractive device, only one-half of the tractive device width needs to be modeled. The simulated loading was applied along the top boundary from the axis of symmetry outward along the

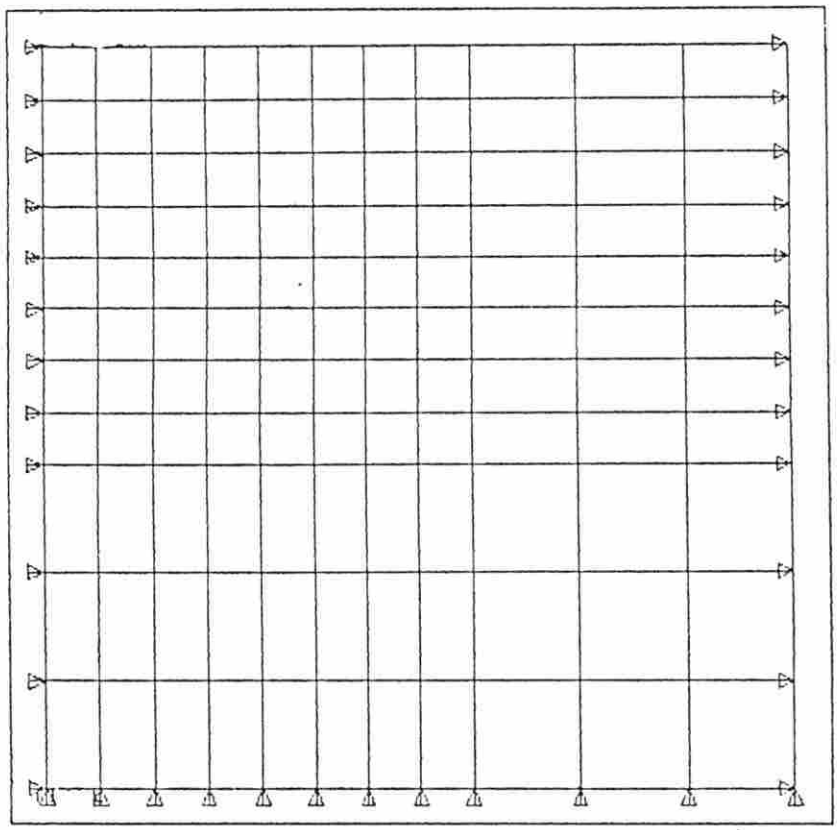

Figure 1. Mesh of rectangular elements used in the finite element model. The origin is at the upper left corner. The x-axis extends in the positve direction along the upper horizontal boundary and represents the soil surface. The y-axis extends in the negative direction along the left, vertical boundary, and represents the plane of symmetry beneath the center of the tractive device. The soil mass is 106.7 cm wide and 106.7 cm deep. The triangles denote rigid boundaries

number of elements needed to model one-half the width of the respective tractive device. The simulated loads are applied along elements that are 7.62 cm wide, the same width as the diameter of the soil samples (described in the next section). This allowed for direct comparison between the predicted bulk densities and measured bulk densities. However, approximate simulated loading widths had to be used in cases where the exact loading width could not be matched to a discrete set of elements.

Four soil layers were included in the model. The first soil layer corresponds to the first two rows of elements, the second layer to the third and fourth rows of elements, and the third layer to the fifth and sixth rows of elements. The fourth layer consists of the remaining five rows of elements because it was assumed that the soil properties will not change beyond a depth of 61 cm.

The type of element employed in the model is the two-dimensional isoparametric solid element (known as STIF42 in ANSYS). The element is defined by four nodal points having two degrees of freedom, translations in the horizontal and vertical directions, at each node. A unit thickness was assumed for the elements in the model.

The nonlinear, elastic-plastic properties were input into the model by means of a stress-strain curve. Up to five points in addition to the origin can be specified to establish the piece-wise linear stress-strain relationship. The program linearly interpolates between the points to determine the value of strain for a given value of stress. The slope of the curve from the origin to the first data

point is assumed by the program to be the modulus of elasticity. Geometrical nonlinearity is also included by employing the large displacement option.

Soil bulk density and Poisson's ratio were also included in the model. The bulk density values were input as gravity loads, by applying the acceleration due to gravity. The values of soil bulk density, along with the stress-strain relationships, were determined experimentally, as described in the next section. Determining a value for Poisson's ratio is difficult to do experimentally. Poisson's ratio for all engineering materials ranges from 0 to 0.5. In the case of soil it is closer to the upper limit of 0.5 (Spangler and Handy, 1982). For the model, Poisson's ratio is assumed to be equal to 0.4.

Evaluation of the Model

Table 1 lists four of the tractors currently being studied in a soil compaction experiment in southeast Iowa. Treatments 1 and 2 are TTTs while treatments 3 and 4 are WTTs. The four tractors are shown in Figures 2 through 5. These treatments correspond to treatments 11, 4, 5, and 6, respectively, in the soil compaction study (Figure A.1, Appendix A). The purpose of the experiment is to study how the different tractor treatments, when used for secondary tillage, affect soil properties and crop growth. Trafficked and untrafficked portions of the individual test plots are monitored to determine the effects of compaction upon soil and plant parameters. (Figure A.2,

Table 1. Tractor data

Tractor Treatment	Type	Force	Track Width	Track Length	Tire or Track Pressure
		KN	------cm------		kPa
1. MPSPL Steel	TTT[a]	127.7	101.6	350.5	17.9
2. 855 Belt	TTT	134.2	61.0	268.0	41.4
3. IH 2+2 Bias	WTT[b]	78.0	50.2	NA	103.4
4. IH 2+2 Terra	WTT	79.6	99.1	NA	48.3

[a]Track type tractor.

[b]Wheel type tractor.

Appendix A). The soil type is a Chequest silty clay loam as classified by the Soil Conservation Service (Raper and Erbach, 1985). The soil properties are listed in Table 2.

Table 2. Soil sample analysis

Sand	Silt	Clay	Organic Matter	Specific Surface
----------%----------				m^2/g
38.4	33.5	28.1	2.2	74.53

The finite element model was used to predict the soil compaction caused by the tractors listed in Table 1. To accurately model the soil it was necessary to determine soil properties as they exist in the field. This required a method to measure the soil in its

Figure 2. Tractor treatment 1: MPSPL Steel

Figure 3. Tractor treatment 2: 855 Belt

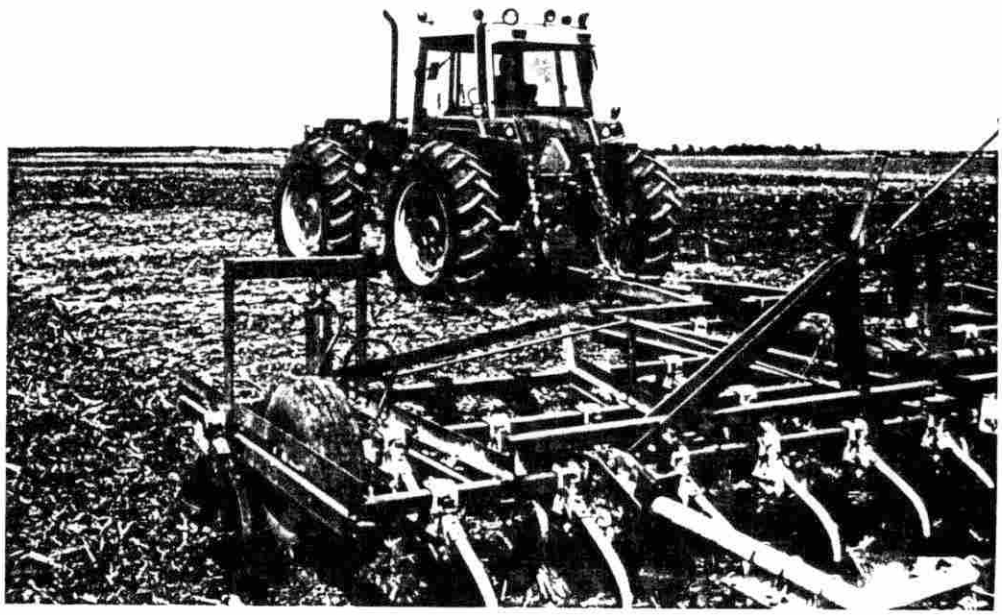

Figure 4. Tractor treatment 3: IH 2+2 Bias

Figure 5. Tractor treatment 4: IH 2+2 Terra

undisturbed state. Soil samples were obtained by means of a tractor mounted soil core sampler (Figure 6).

Determination of Soil Properties

The stress-strain relationships for the model were determined from soil samples that were obtained from the plots just before the compaction treatments were applied, on June 2, 1986. Three replications of cores were taken for each tractor treatment, one core from each of the individual treatment test plots in the first three replications of the field experiment (Figure A.1, Appendix A). The soil cores were taken to a depth of 61 cm. Four samples of equal size, 15.2 cm in length and 7.6 cm in diameter, were removed from each core. This allowed for stress-strain relationships to be determined for four soil layers.

The soil samples were removed from the soil core tube in steel rings. Tin foil was wrapped around each open end of the rings and secured with rubber bands. The samples were then placed into Ziploc plastic bags that were sealed to prevent moisture loss. This procedure provided a means of transporting and testing the samples in their original undisturbed state.

Figure 7 shows the Instron Model 1125 Universal Testing Instrument that was used to determine the soil stress-strain relationships. It consists of a crosshead drive system, that loads soil samples, and a load weighing system that detects and records the applied loads and the soil strain.

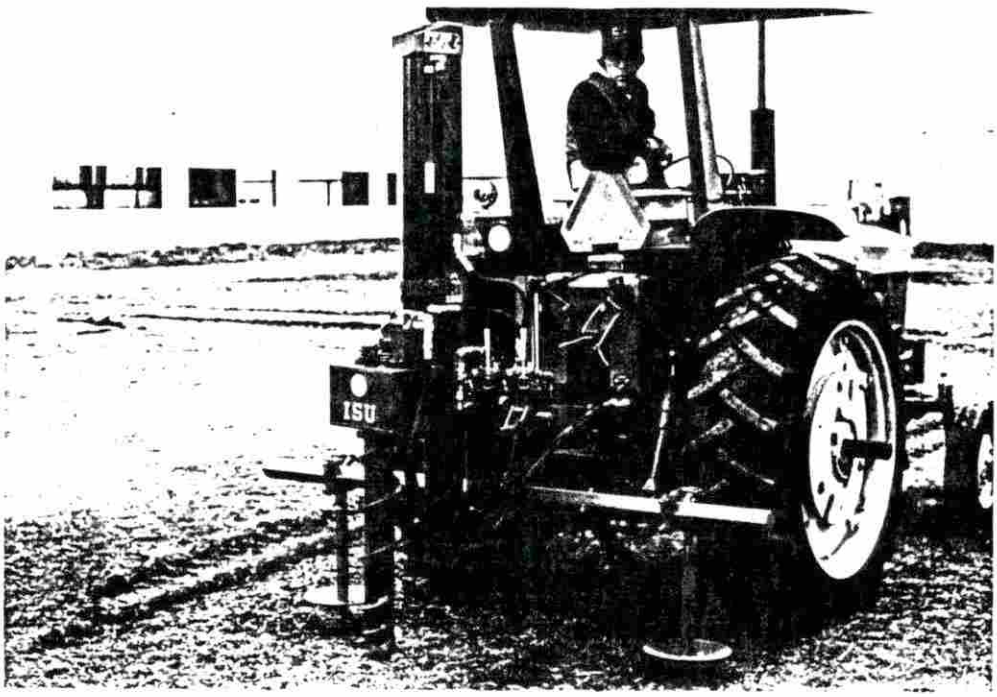

Figure 6. Tractor mounted soil core sampler

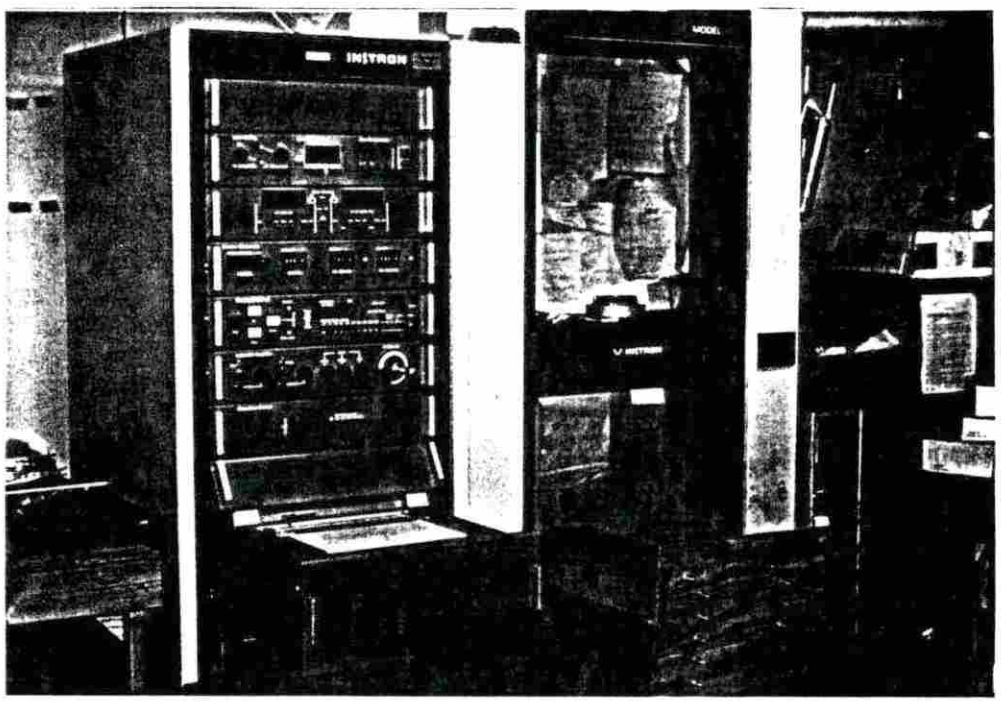

Figure 7. Instron Model 1125 Universal Testing Instrument with crosshead drive system (on left) and load weighing system (on right)

The soil samples were loaded in compression by means of a 2.54 cm diameter aluminum piston attached to a load cell, mounted on the loading crosshead (Figure 8). As can be seen in Figure 8, the soil samples were contained in the steel sampling rings during the compression tests, which constrained movement in the lateral direction. Air gaps were present between the ring wall and the soil because the diameter of the rings was slightly larger than the diameter of the soil samples (Figure 9). Therefore, fine sandblasting sand was poured into the gaps between the ring and the soil to maintain the uniform confining effect (Figure 10). It was felt that the sandblasting sand would have negligible influence upon th soil during the test.

The reason for using a piston with a smaller diameter than that of the soil samples is that when a vehicle load is applied to the soil, the soil in the immediate vicinity of contact is not totally confined, and there is usually some plastic flow. However, the soil resistance to deformation increases as penetration increases, until no more soil deformation occurs. Thus, the goal of the compression test used in this study was to simulate this kind of phenomenon.

The rate of loading employed in the compression tests was 2 cm/min. This is obviously very slow when compared to the rate of loading of a tire or a track but the loading rate was limited by the capabilities of the Instron testing instrument. The samples were loaded to a maximum of 10 kg, which corresponds to a maximum pressure of 193.7 kPa.

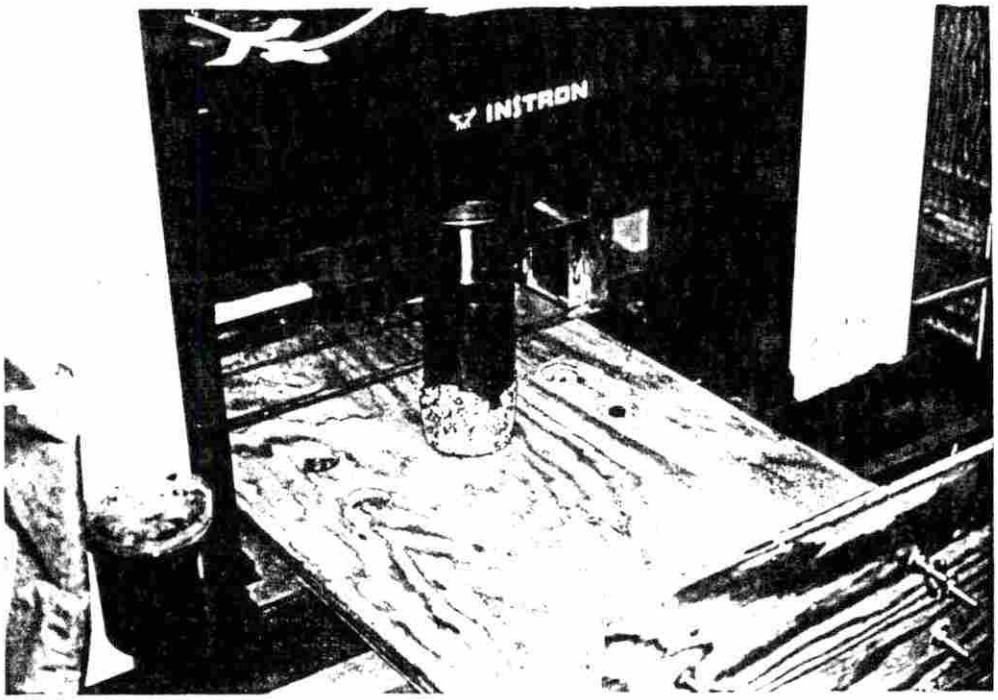

Figure 8. Compression test with 2.54 cm diameter aluminum piston

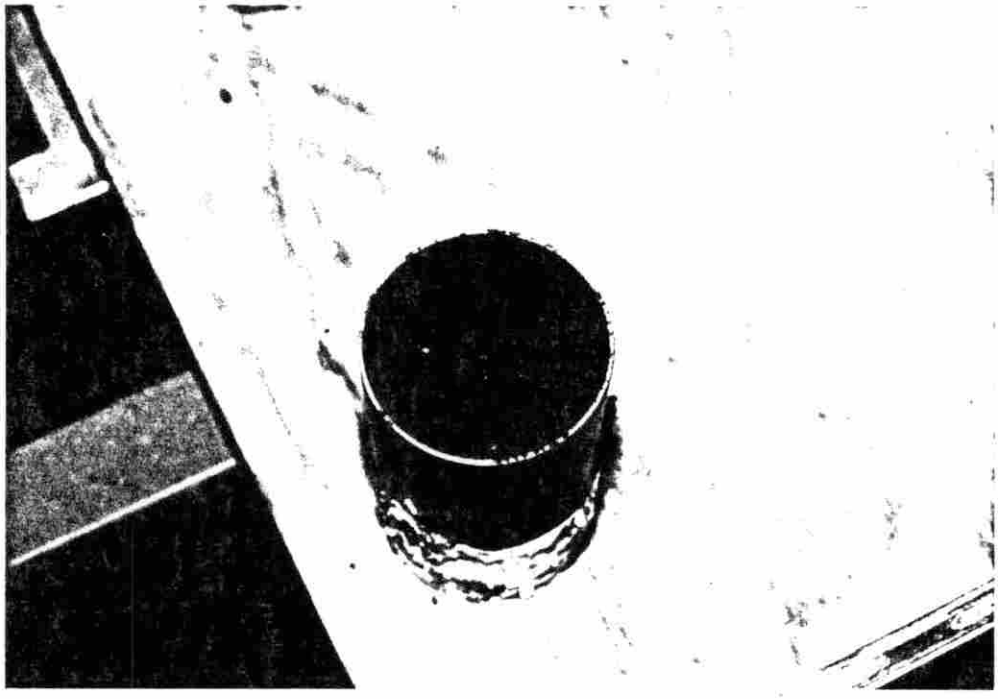

Figure 9. Air gap present between steel ring and soil sample

Figure 10. Sandblasting sand being poured into air gap between steel ring and soil sample

The bulk densities of the soil layers were determined from samples collected on June 16, 1986. Soil cores were taken to a depth of 66.04 cm for the trafficked and untrafficked portions of each test plot. The 7.62 cm diameter cores were sectioned into 13 samples, 5.08 cm long (only the first twelve samples were used in the study). For the soil layers in the model, the bulk density value input for each layer was assumed to be equal to the average of the bulk densities measured for the corresponding three samples of untrafficked soil. These bulk density values were the average values determined for all four treatments. The bulk density values predicted by the model after a load was applied were compared to the average value of bulk density measured for the corresponding three samples of trafficked soil. The measured bulk density values for the trafficked soil were also the the average values determined for all four treatments.

RESULTS AND DISCUSSION

Soil Parameters Measured

The results of the soil compression tests are shown in Figures 11 through 15. Figures 11 through 14 are the stress-strain relationships determined for tractor treatments 1 through 4 respectively. Figure 15 shows the average stress-strain relationships for the four tractor treatments.

Each of the figures clearly shows an increase in soil strength down to the third layer. The third and fourth layers have nearly identical strength characteristics. The soil strength profile reflected that the field where the test plots are located was moldboard plowed to a depth of approximately 25 cm (10 in) the previous fall. This tillage would have loosened the upper two soil layers but did not affect the lower two layers.

During the compression tests, the piston easily penetrated the soil samples from the first layer, resulting in large plastic deformation. Plastic deformation occurred during the compression of the samples from the second soil layer, but the piston penetration was not as deep. The soil from the lower two layers was strong enough so that very little plastic deformation occurred.

Some of the curves in Figures 11 through 15 show a low initial soil strength. With further piston penetration into the samples, soil strength increased. The slopes of the stress-strain curves are then linear or steadily decrease. This was most noticeable for the

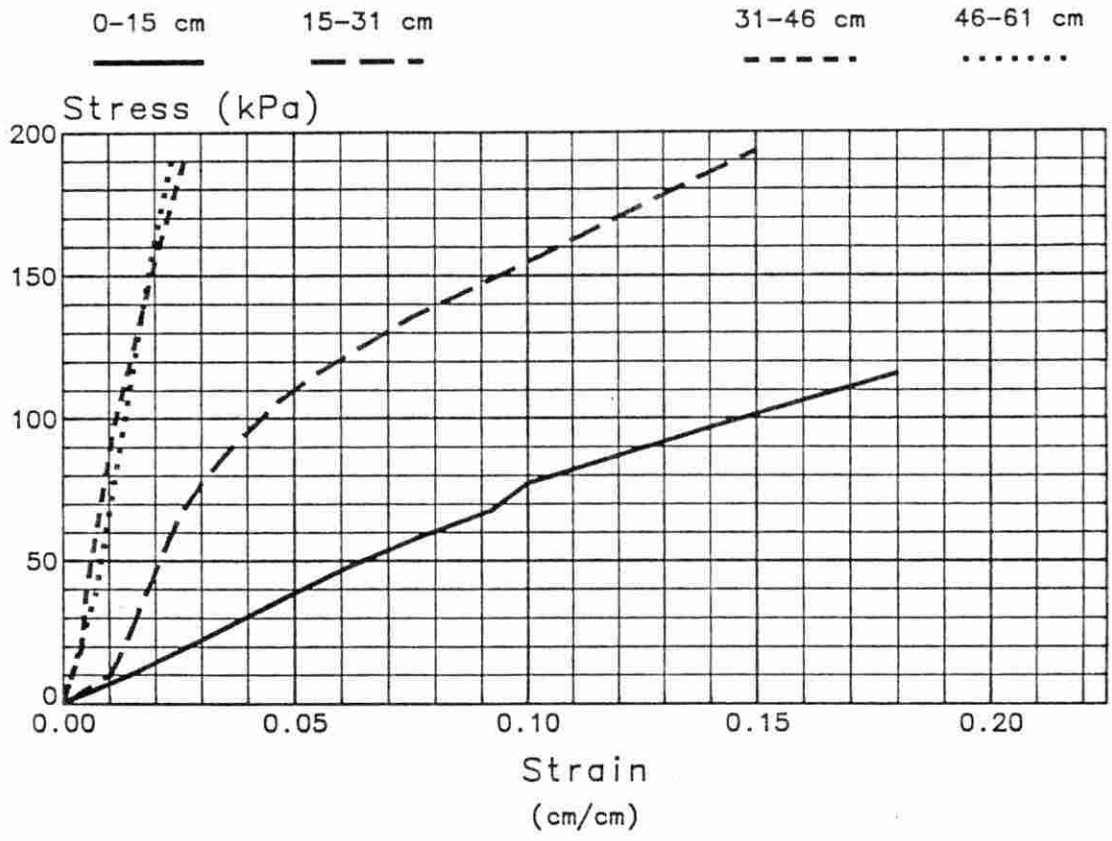

Figure 11. Stress-strain relationships determined for four depths of untrafficked soil in plots trafficked with the MPSPL Steel TTT (treatment 1, Table 1)

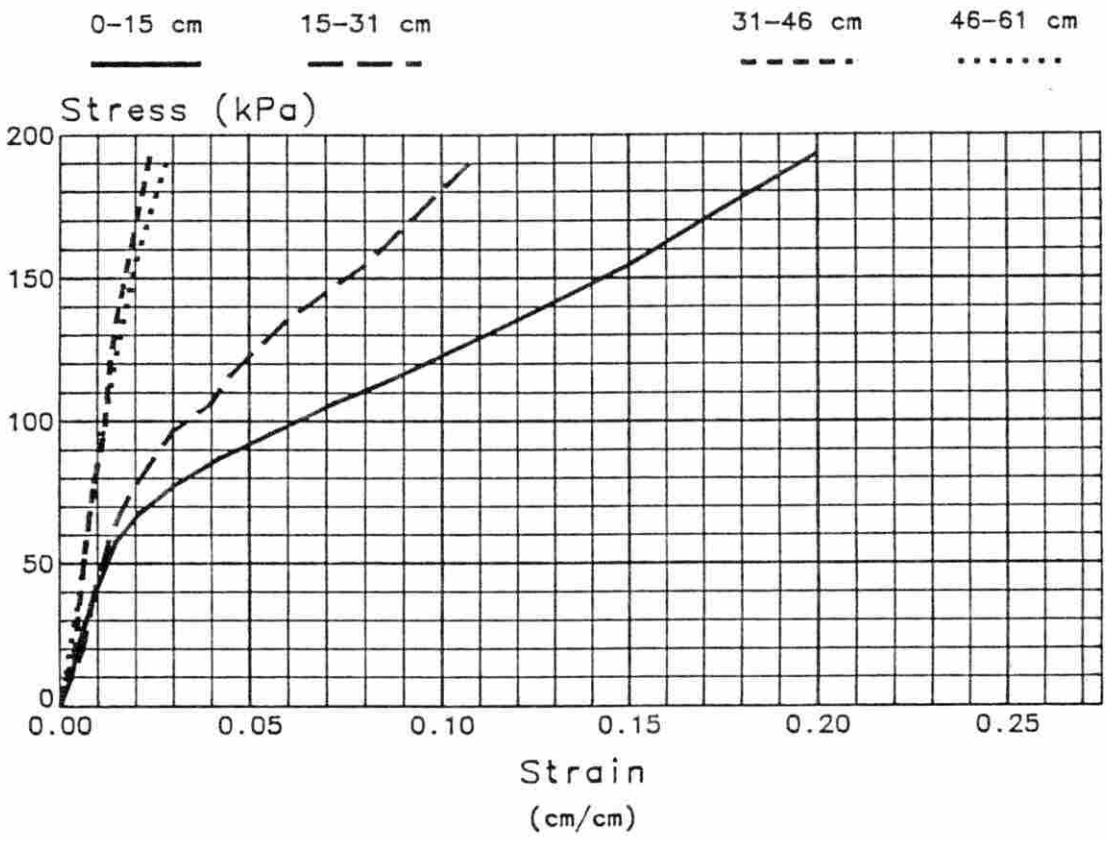

Figure 12. Stress-strain relationships determined for four depths of untrafficked soil in plots trafficked with the 855 Belt TTT (treatment 2, Table 1)

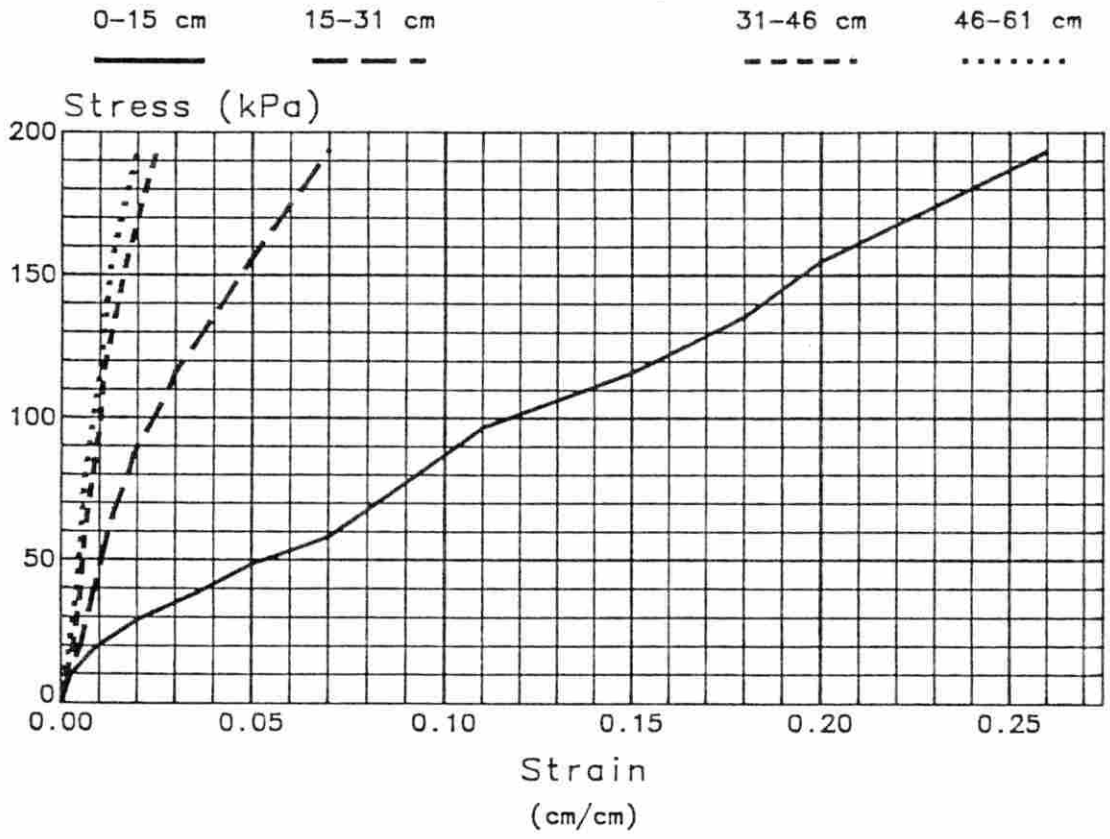

Figure 13. Stress-strain relationships determined for four depths of untrafficked soil in plots trafficked with the IH 2+2 Bias WTT (treatment 3, Table 1)

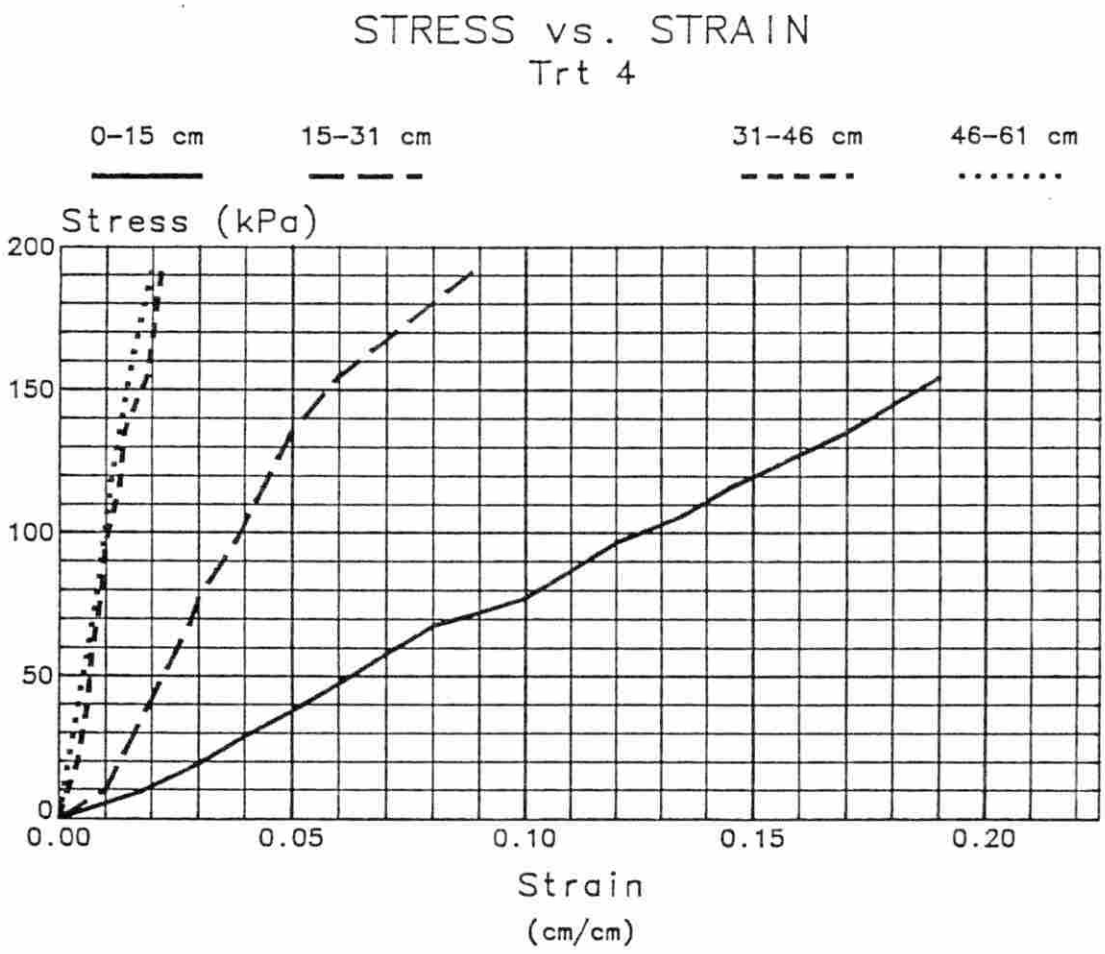

Figure 14. Stress-strain relationships determined for four depths of untrafficked soil in plots trafficked with the IH 2+2 Terra WTT (treatment 4, Table 1)

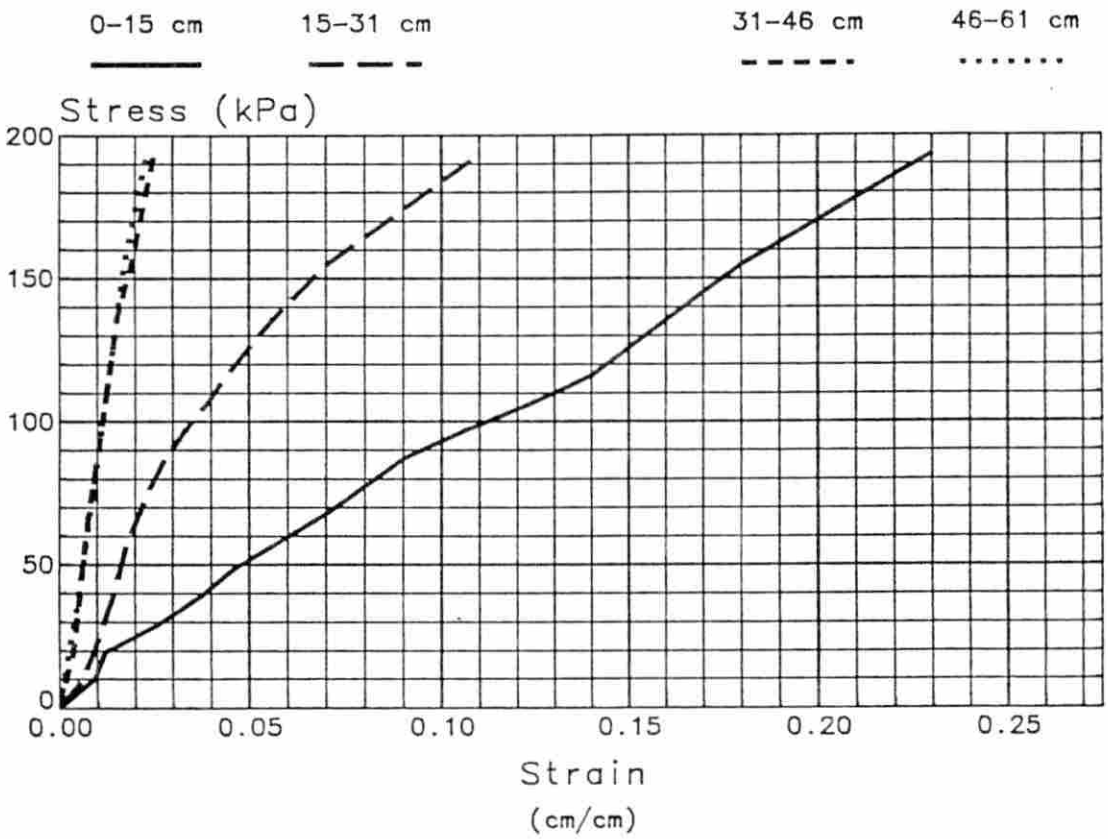

Figure 15. Average stress-strain relationships for four depths of untrafficked soil for all four treatments

upper two soil layers.

One possible reason for the low initial soil strength is the uneven soil surface present in many of the samples. It is possible that only part of the piston face was initially in contact with the soil, resulting in less soil resistance at first. Another possible reason is that voids and cracks in the soil samples could result in lower soil resistance at first. It is also possible that the trend indicates some type of soil hardening behavior.

The stress-strain relationships in Figures 11 through 14 reflect the variability that exists in the undisturbed soil samples. Much of the variability can be attributed to variability in soil conditions in the field. Figure 16 shows the confidence intervals for one standard deviation determined from the average stress-strain data.

For the stress-strain relationships in the model, the average values for the four treatments (Figure 15), were used. The average stress-strain relationships were chosen because of the variability present in the stress-strain relationships determined for the indvidual treatments. ANSYS constraints required that points had to be chosen on the curves so that the slope for each succesive piecewise line segment was less than the previous one. Therefore, the low initial soil strength mentioned previously was ignored for the layered soil model.

The layered soil properties before compaction are listed in Table 3. The untrafficked bulk density and soil moisture content values are averages determined for the four treatments. The modulus

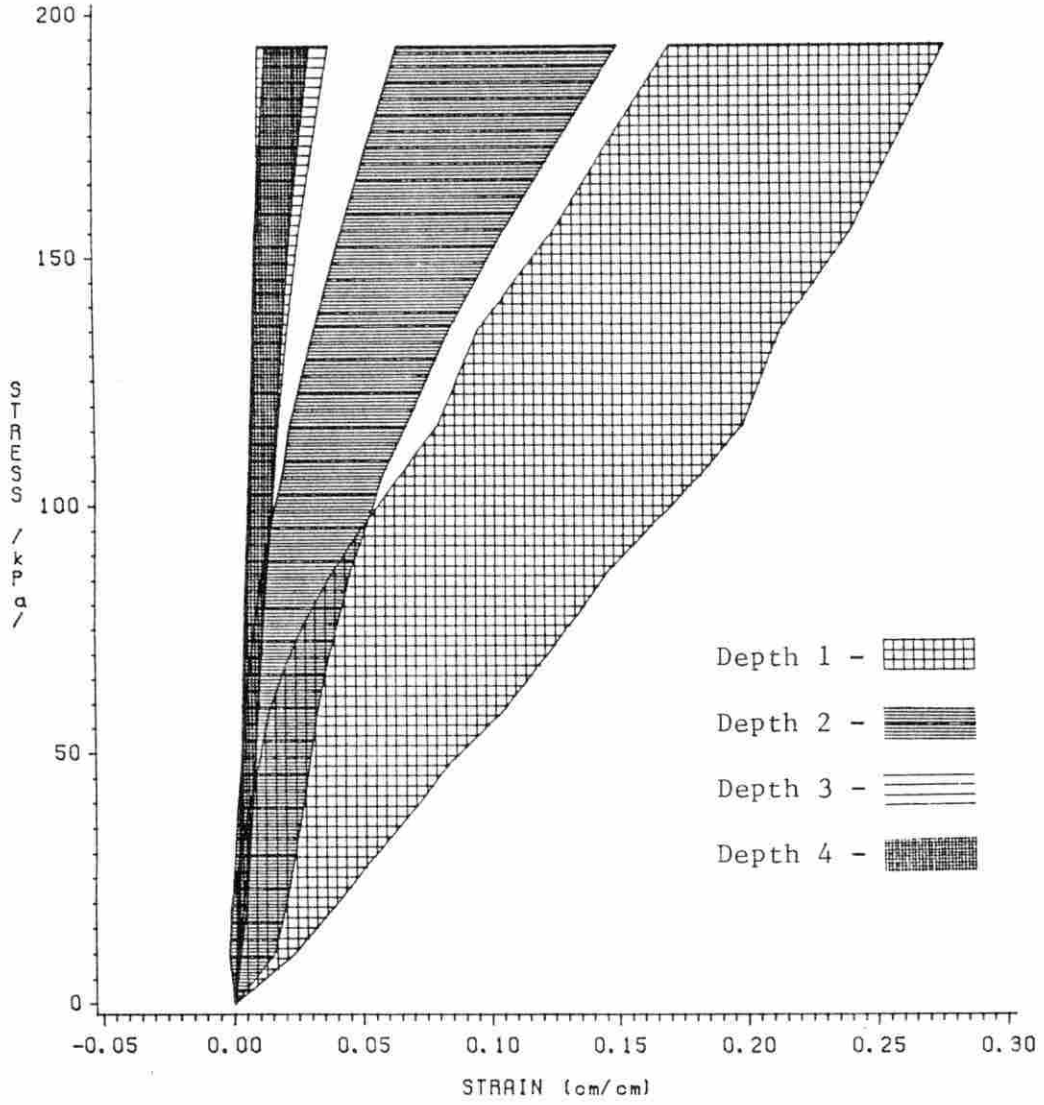

Figure 16. Confidence intervals of one standard deviation for the average stress-strain data

Table 3. Properties of soil layers as affected by depth

Depth	Modulus of Elasticity	Bulk Density		Soil Moisture[a]	
		mean	s.d.[b]	mean	s.d.[b]
cm	kPa	----Mg/m^3----		------%------	
0-15	1611	1.14	0.09	23.81	3.62
16-31	3223	1.53	0.05	25.46	2.70
31-46	9024	1.61	0.07	22.76	5.85
46-61	9100	1.62	0.07	23.66	3.92

[a]Soil moisture was not used in the model.

[b]Standard deviation.

of elasticity values and the bulk density values show the increasing soil strength down to the third layer. The soil moisture contents were not input into the model.

Soil Strain and Bulk Density Changes Predicted by Model

Figures 17 through 21 show examples of strain contours predicted by the model. Figures 17 and 18 are the elastic horizontal- and vertical-strain contours predicted for the loading by the IH 2+2 Bias (treatment 3). Figures 19 and 20 are the plastic horizontal- and vertical-strain contours predicted for the treatment 3 loading. Figure 21 is the elastic vertical-strain contours predicted for the loading by the MPSPL Steel (treatment 1).

The maximum negative strains (MN) and maximum positive strains

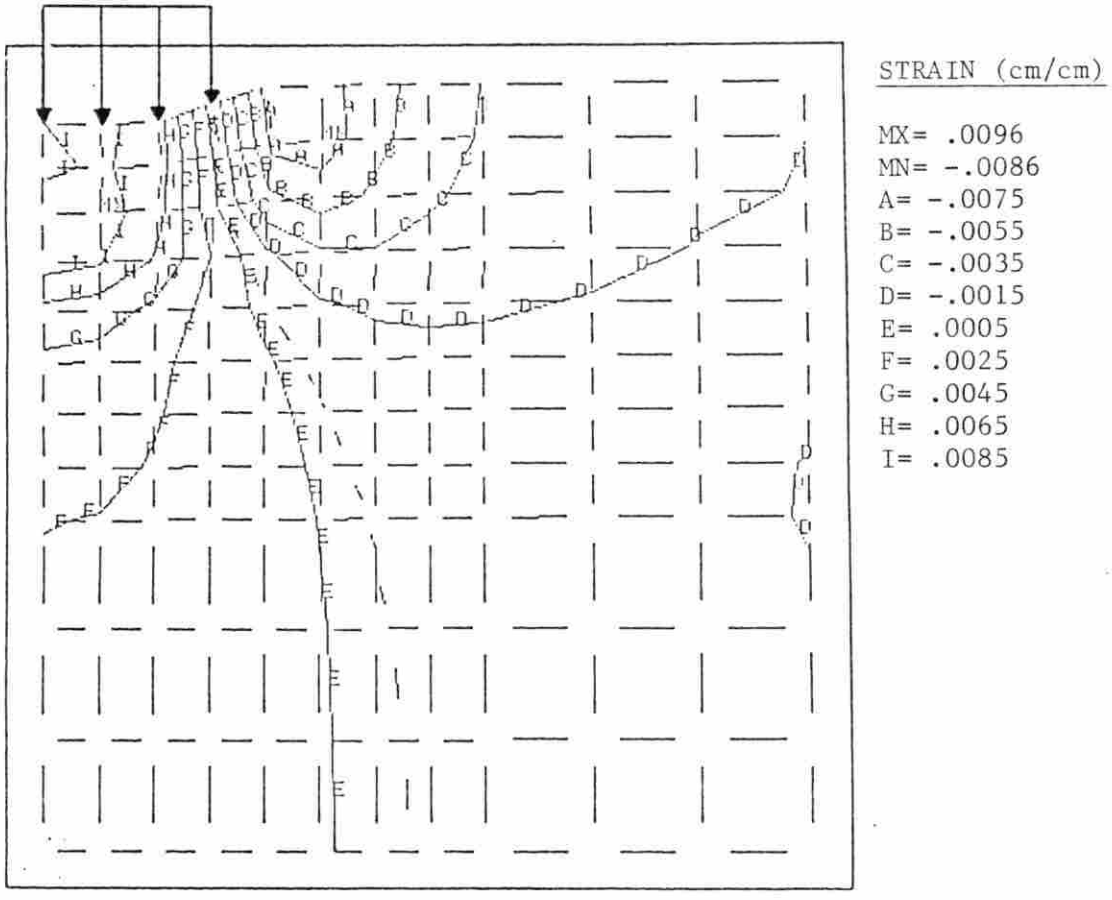

Figure 17. Elastic horizontal-strain contours predicted for the IH 2+2 Bias (treatment 3, Table 1). A pressure of 103.4 kPa was applied along three elements. The values for the strain contours and the maximum positive (MX) and maximum negative (MN) strains are listed on the right

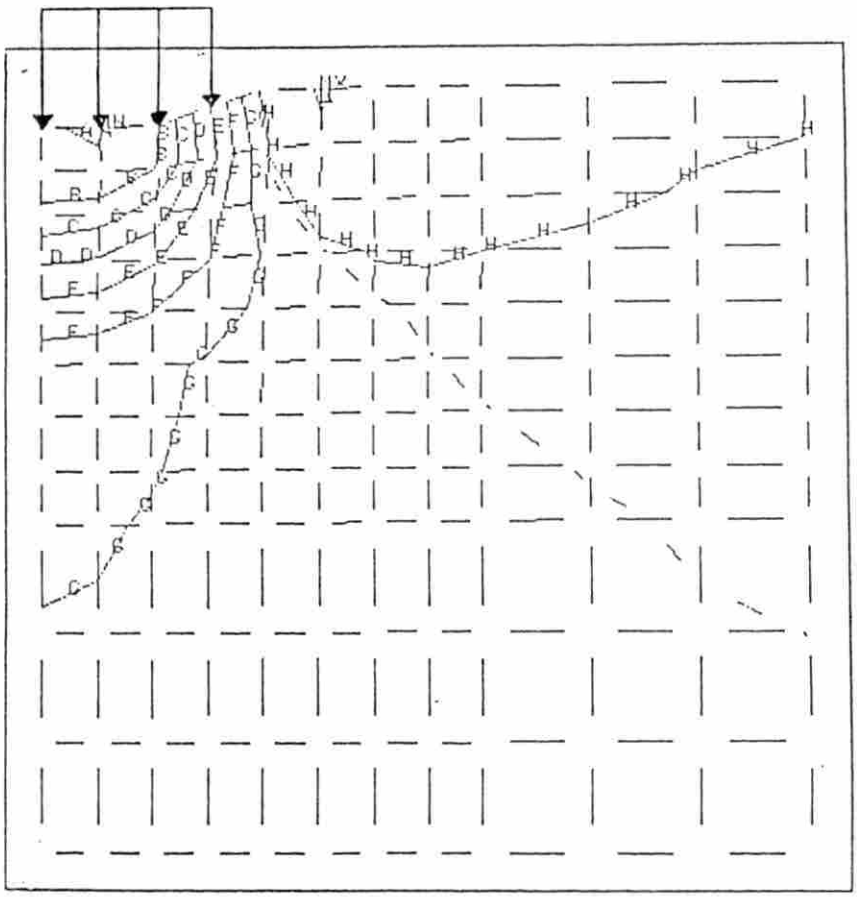

STRAIN (cm/cm)

MX= .0061
MN= -.035
A= -.034
B= -.029
C= -.024
D= -.019
E= -.014
F= -.0093
G= -.0043
H= .0007
I= .0057

Figure 18. Elastic vertical-strain contours predicted for the IH 2+2 Bias (treatment 3, Table 1). A pressure of 103.4 kPa was applied along three elements. The values for the strain contours and the maximum positive (MX) and maximum negative (MN) strains are listed on the right

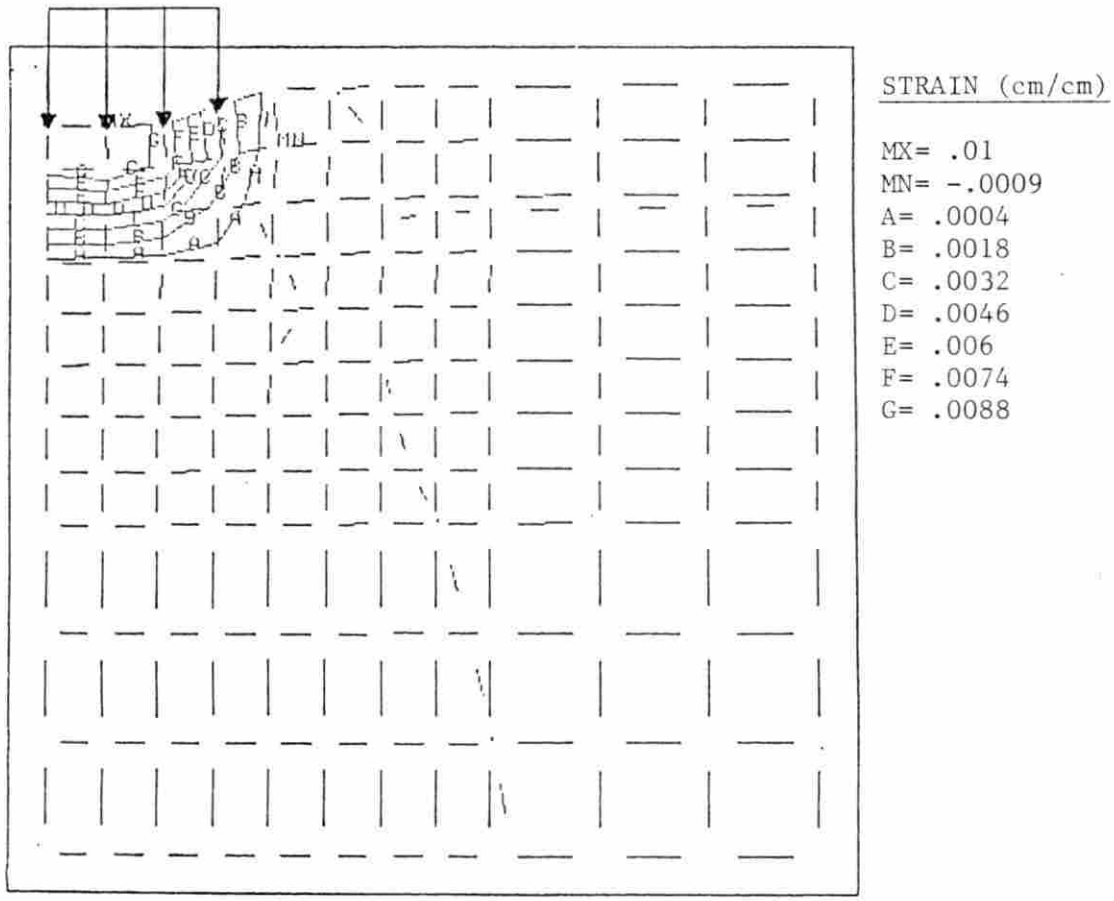

Figure 19. Plastic horizontal-strain contours predicted for the IH 2+2 Bias (treatment 3, Table 1). A pressure of 103.4 kPa was applied along three elements. The values for the strain contours and the maximum positive (MX) and maximum negative (MN) strains are listed on the right

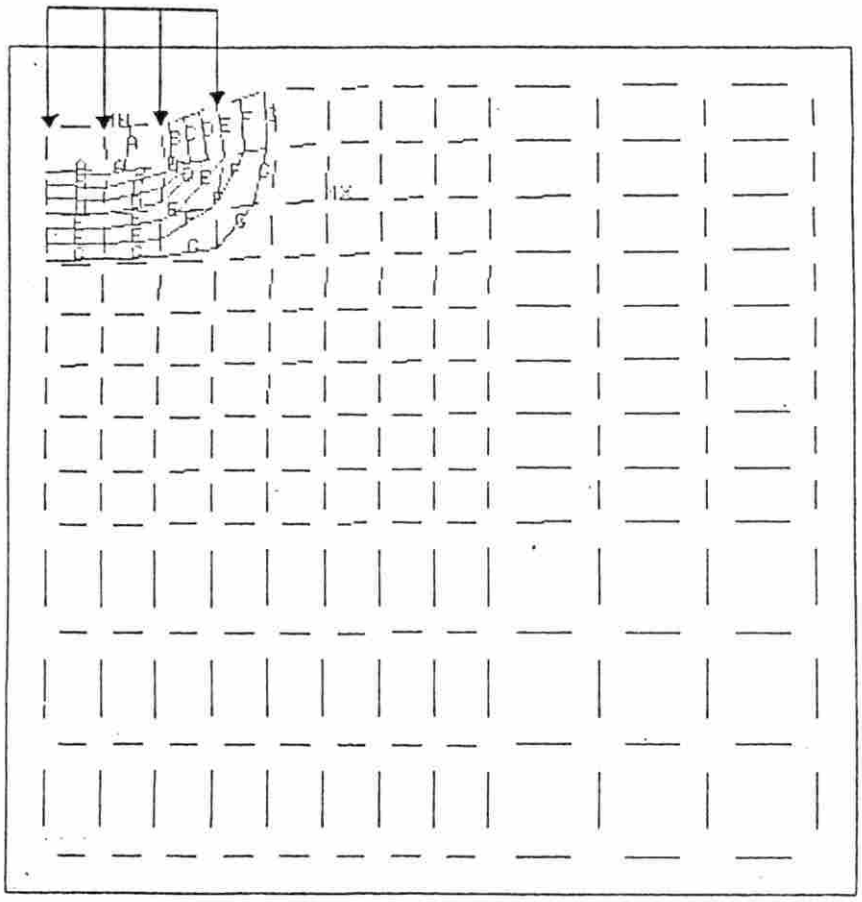

Figure 20. Plastic vertical-strain contours predicted for the IH 2+2 Bias (treatment 3, Table 1). A pressure of 103.4 kPa was applied along three elements. The values for the strain contours and the maximum positive (MX) and maximum negative (MN) strains are listed on the right

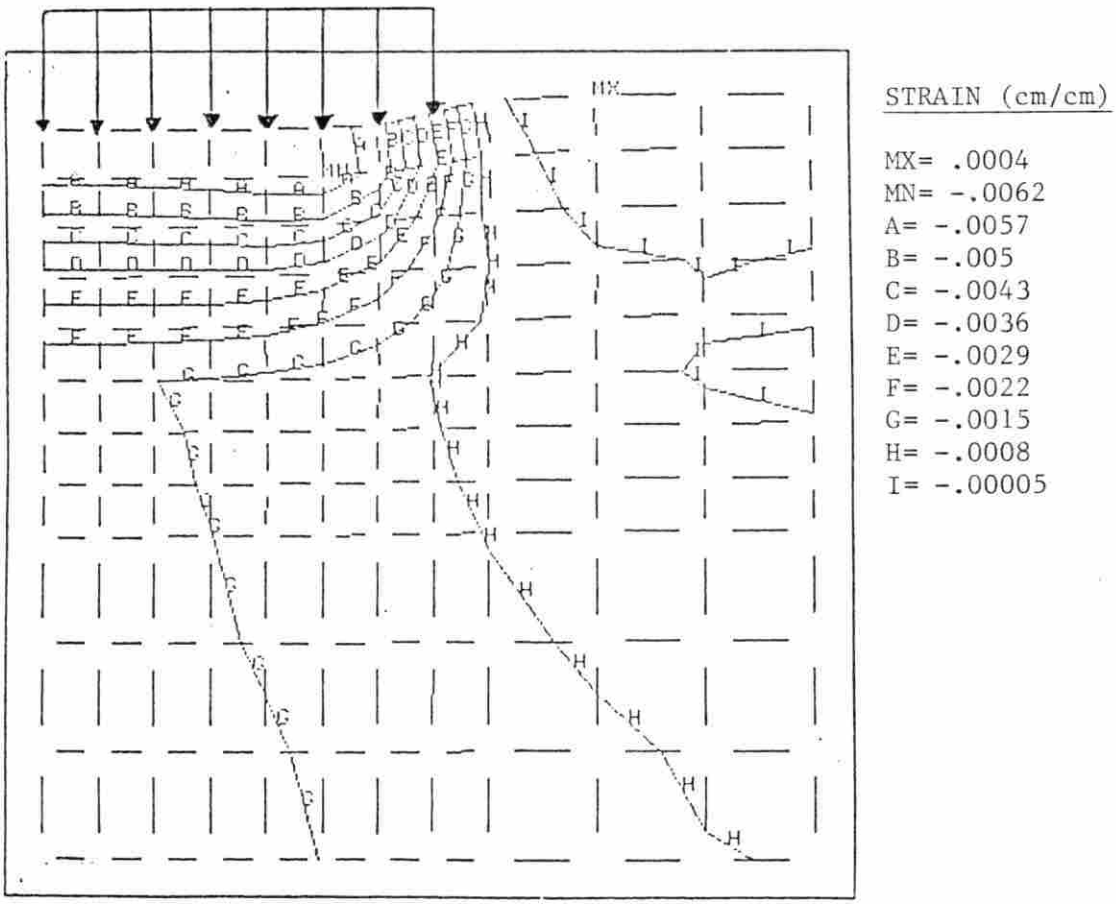

Figure 21. Elastic vertical-strain contours predicted for the MPSPL Steel (treatment 1, Table 1). A pressure of 17.9 kPa was applied along seven elements. The values for the strain contours and the maximum positive (MX) and maximum negative (MN) strains are listed on the right

(MX) are shown in Figures 17 through 21. In some cases the maximum strains occurred at the soil surface while in others they occurred at some finite depth.

The model predicted that only elastic strain occured for the simulated loading for the MPSPL Steel, 855 Belt, and the IH 2+2 Terra (treatments 1, 2, and 4 respectively). The plastic strain predicted for the IH 2+2 Bias (treatment 3) was smaller than that calculated for the elastic strain. This indicates that a large amount of soil rebound would be expected upon unloading. However, previous research indicates that most agricultural soils experience little rebound upon unloading. Johnson et al. (1984) applied hydrostatic stress to loose soil samples of Lloyd clay with a triaxial device. The soil experienced little rebound in the tests, and the majority of strain was plastic. Stone and Larson (1980) studied the rebound of five agricultural soils using a uniaxial compression tester. The decrease in bulk density was usually less than 0.05 Mg/m^3 after the removal of stress.

Because soil rebounds very little, it was assumed that both the elastic and plastic strain experienced by the soil in the model was permanent. Thus, the model results were compared to those measured in the field on the basis of total strain. Table 4 lists the bulk densities predicted for the four treatments and the measured bulk densities for the four soil layers. The measured bulk densities are the average values determined from the trafficked soil for the four treatments. The predicted bulk densities were determined from the

Table 4. Predicted versus measured bulk densities for the layered soil

Depth	Predicted Bulk Density				Measured Bulk Density[a]	
	Trt 1	Trt 2	Trt 3	Trt 4[b]	mean	s.d.[c]
cm	---------- Mg/m^3 ----------					
0-15	1.15	1.15	1.17	1.16	1.27	0.09
15-31	1.53	1.54	1.55	1.54	1.53	0.08
31-46	1.61	1.61	1.61	1.61	1.60	0.08
46-61	1.62	1.62	1.63	1.62	1.59	0.09

[a]Average bulk densities determined for all four treatments.

[b]Trt 1 = MPSPL Steel, Trt 2 = 855 Belt, Trt 3 = IH 2+2 Bias, Trt 4 = IH 2+2 Terra.

[c]Standard deviation.

elements adjacent to the boundary of symmetry, because those elements are closest to the center of the tractive device.

Table 4 shows that the bulk density predictions for the first layer were much less than the measured value for all four treatments. It could be expected that the model would predict lower bulk densities for lower applied pressures, however, field measurements indicate that the bulk densities in the upper soil layer lie between 1.22 and 1.32 Mg/m^3 for these treatments. This indicates that the model definitely under predicts the amount of compaction occurring in the top layer of soil. The predicted values were close to the measured values for the remaining three soil layers. The

measured values for the lower two soil layers were less than the corresponding values (Table 3) measured for the untrafficked soil. This shows the variability of the soil in the field.

One possible reason for the low values predicted by the model is the assumption that the load is the nominal mean ground pressure for the TTTs and the inflation pressure for the WTTs. Past research indicates that peak stresses applied by a tire or track may be much higher than the nominal mean ground pressure or the inflation pressure. Plackett (1984) measured the stresses beneath several different tires on a smooth surface. He found that the peak ground pressure exceeded the mean ground pressure by a factor of from 2 to 2.6. Vandenberg and Gill (1962) measured the interface stresses that develop in the soil beneath a tractor tire. They tested a 11-38 four-ply tractor tire at three inflation pressures and found that the maximum pressures recorded were at least twice the average inflation pressure. Kogure and Sugiyama (1975) measured the ground pressure beneath a TTT at a depth of 15 cm below the soil surface. They found that the mean maximum ground pressure was 2.75 times larger than the nominal mean ground pressure.

In order to simulate peak pressure loading, a pressure equal to 206.8 kPa, twice that of the IH 2+2 Bias (treatment 3) contact pressure, was applied along three elements in the model. The elastic vertical-strain contours and plastic vertical-stain contours are shown in Figures 22 and 23, respectively. The maximum negative vertical-strain(MN) predicted was located at the soil surface in

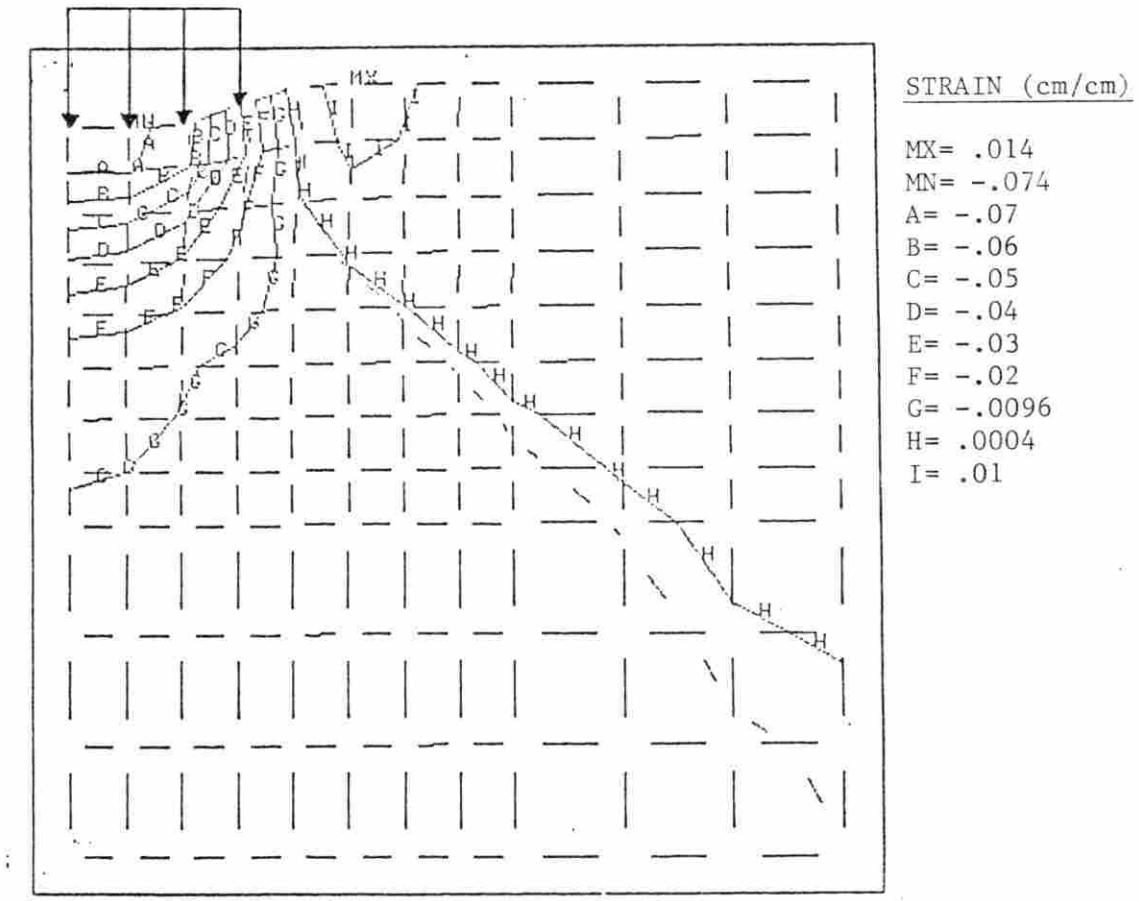

Figure 22. Elastic vertical-strain contours for the simulated higher pressure for the IH 2+2 Bias (treatment 3, Table 1). A pressure of 206.8 kPa was applied along three elements. The values for the strain contours and the maximum positive (MX) and maximum negative (MN) strains are listed on the right

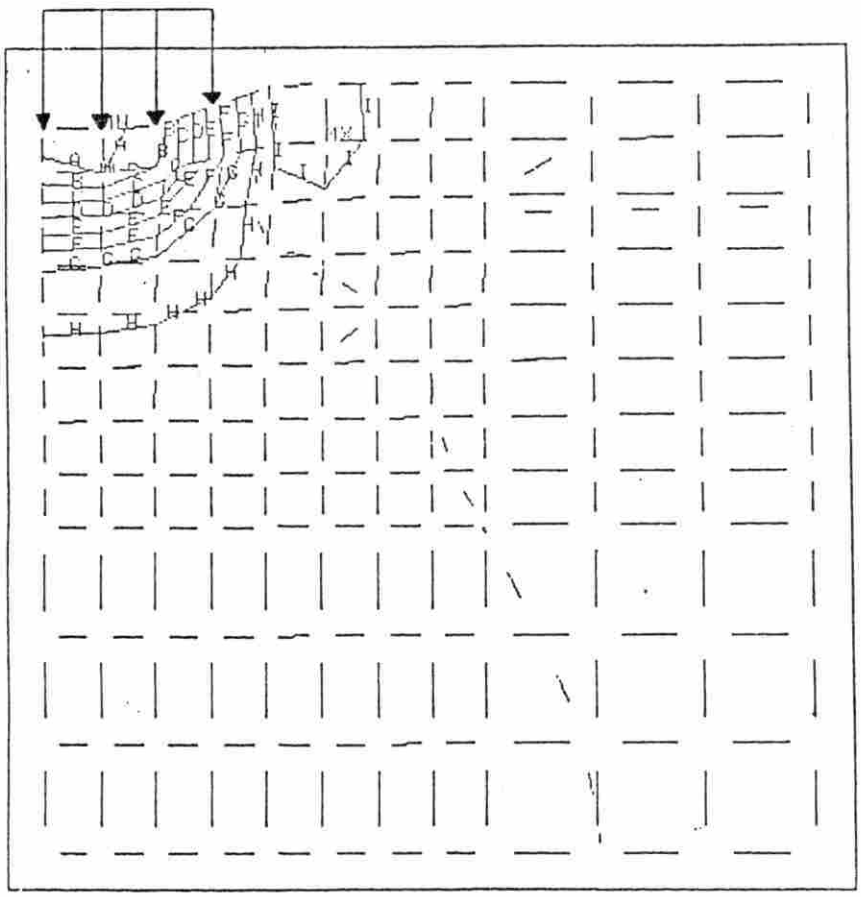

Figure 23. Plastic vertical-strain contours for the simulated higher pressure for the IH 2+2 Bias (treatment 3, Table 1). A pressure of 206.8 kPa was applied along three elements. The values for the strain contours and the maximum positive (MX) and maximum negative (MN) strains are listed on the right

both cases. The contours are similar to those predicted for the IH 2+2 Bias (treatment 3) nominal pressure loading, but the magnitude of the strains are greater.

Table 5 compares the predicted bulk densities for both the

Table 5. Predicted bulk densities of the layered soil versus measured values for the IH 2+2 Bias (treatment 3) low and high loadings

Depth	Predicted Bulk Densities				Measured Bulk Density[a]	
	low load	diff[b]	high load	diff[b]	mean	s.d.[c]
cm	Mg/m^3	%	Mg/m^3	%	----Mg/m^3----	
0-15	1.17	-7.87	1.21	-4.72	1.27	0.09
15-31	1.55	1.31	1.56	1.96	1.53	0.08
31-46	1.61	0.63	1.62	1.25	1.60	0.08
46-61	1.63	2.52	1.63	2.52	1.59	0.09

[a]Average bulk density values for all four treatments.

[b]Percentage difference between predicted and measured values, based on the measured bulk density.

[c]Standard Deviation.

nominal pressure loading and the high pressure loading for IH 2+2 Bias (treatment 3), with the average measured bulk densities for the four soil layers. The predicted bulk densities are based on the total strain calculated for the elements adjacent to the line of symmetry. The table shows the percentage difference between the bulk densities predicted for the two simulated loads and the measured bulk

densities. The bulk density predicted by the higher load for the top layer of soil is closer to the measured value of bulk density. However, it still under predicts the measured bulk density value by a large margin. The model predicted that the higher load would produce a little more compaction in layers two and three.

The model not only lends itself to variations in loading but also to variations in soil type. It was of interest to observe how the model responded when a uniform soil profile was modeled. Table 6 lists the soil coefficients for two different uniform soils, one of

Table 6. Soil coefficients for the uniform soils

Soil Type	Modulus of Elasticity	Bulk Density
	kPa	Mg/m^3
High Strength	4740	1.43
Low Strength	1074	1.14

high strength and one of low strength. The modulus of elasticity and the bulk density for the high strength soil are the average values for the respective coefficients of the layered soil, with the third and fourth layers combined as one layer. The low strength soil was chosen so that its modulus of elasticity was less than the modulus of elasticity for the first layer of the layered soil. The reason for choosing a soil with lower strength was to see if the model predicted higher levels of plastic strain for the low strength soil.

The nominal contact pressure for the IH 2+2 Bias (treatment 3, Table 1) was applied as the simulated load upon both soil types. Figure 24 shows the resulting elastic vertical-strain contours for the high strength soil. Figures 25 and 26 show the elastic vertical-strain contours and the plastic vertical-strain contours, respectively, for the low strength soil. No plastic strain was predicted for the high strength soil. The maximum negative elastic vertical-strain (MN) occurred at approximately 15 cm below the soil surface for both soil types. The maximum negative plastic vertical-strain (MN) for the low strength soil occurred at about 23 cm below the soil surface.

Figures 24, 25, and 26 show that a more uniform distribution of strain was predicted for the uniform soil profiles than for the layered soil. The predicted strain contours for the uniform soils extend to a deeper depth than those predicted for the layered soil. This is especially true for the plastic vertical-strain contours of Figure 26. These results show the effect of removing the lower layers of high strength soil.

Table 7 contains the predicted bulk densities for the two uniform soils. The bulk density values were again calculated on the basis of total strain predicted in the elements adjacent to the boundary of symmetry. The bulk density values were determined for the corresponding layers of elements employed for the layered soil, as a means of comparison. Table 8 shows that little bulk density change occurred for the high strength soil. Greater compaction was

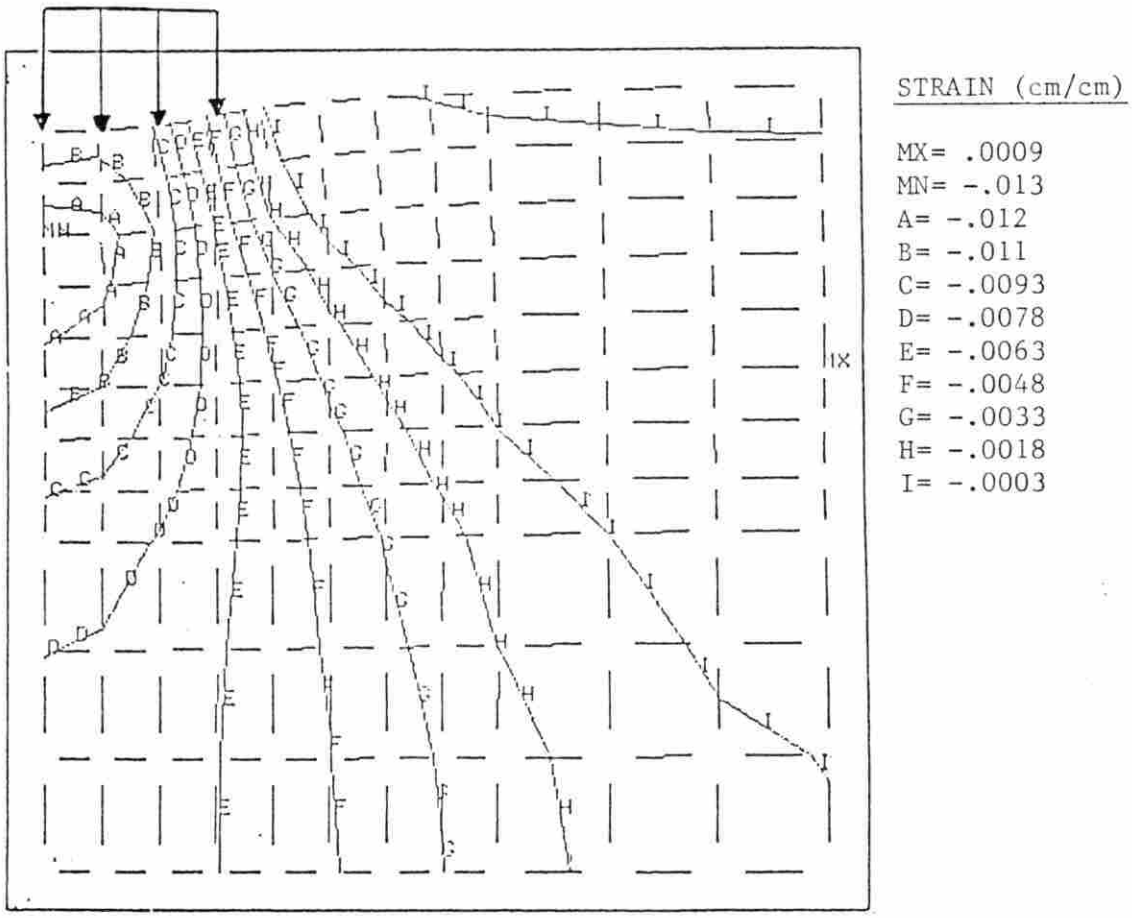

Figure 24. Elastic vertical-strain contours for the uniform high strength soil. Pressure for IH 2+2 Bias (treatment 3, Table 1) of 103.4 kPa applied along three elements. The values for the strain contours and the maximum positive (MX) and maximum negative (MN) strains are listed on the right

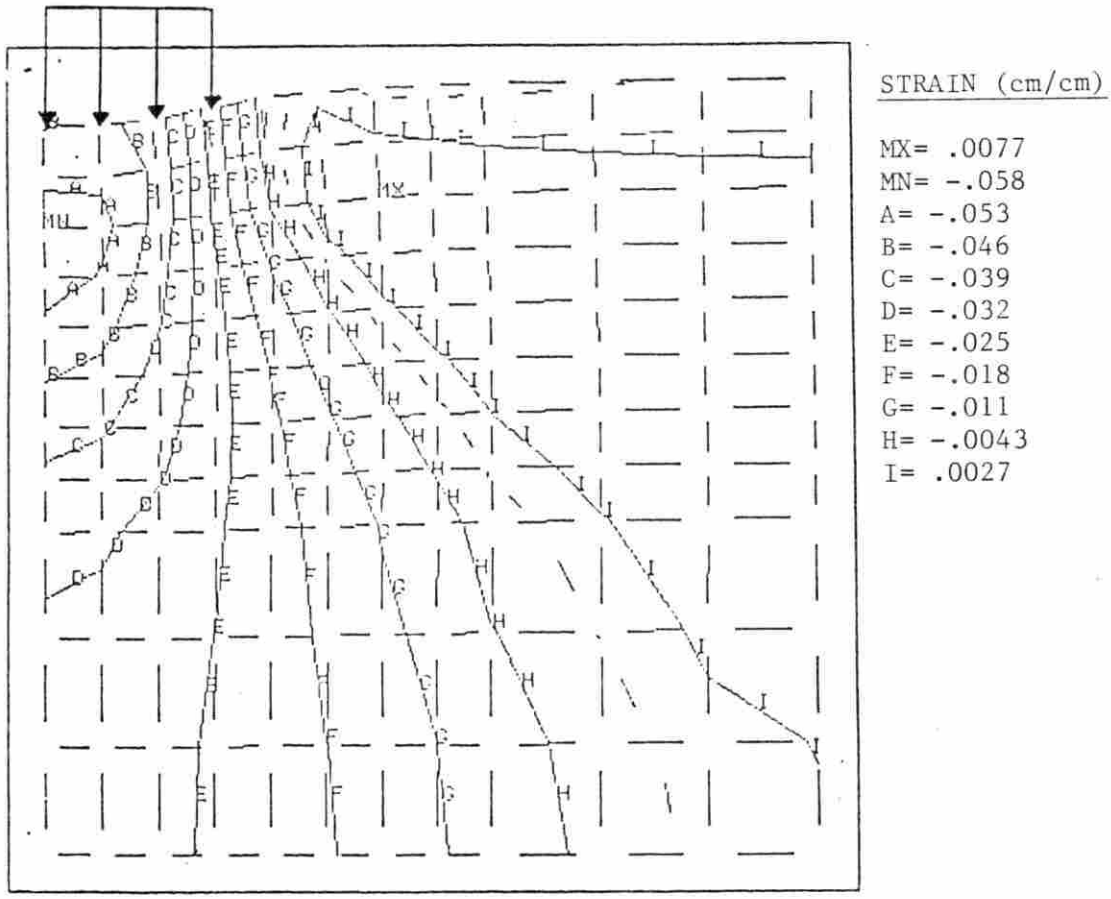

Figure 25. Elastic vertical-strain contours for the uniform low strength soil. Pressure for IH 2+2 Bias (treatment 3, Table 1) of 103.4 kPa applied along three elements. The values for the strain contours and the maximum positive (MX) and maximum negative (MN) strains are listed on the right

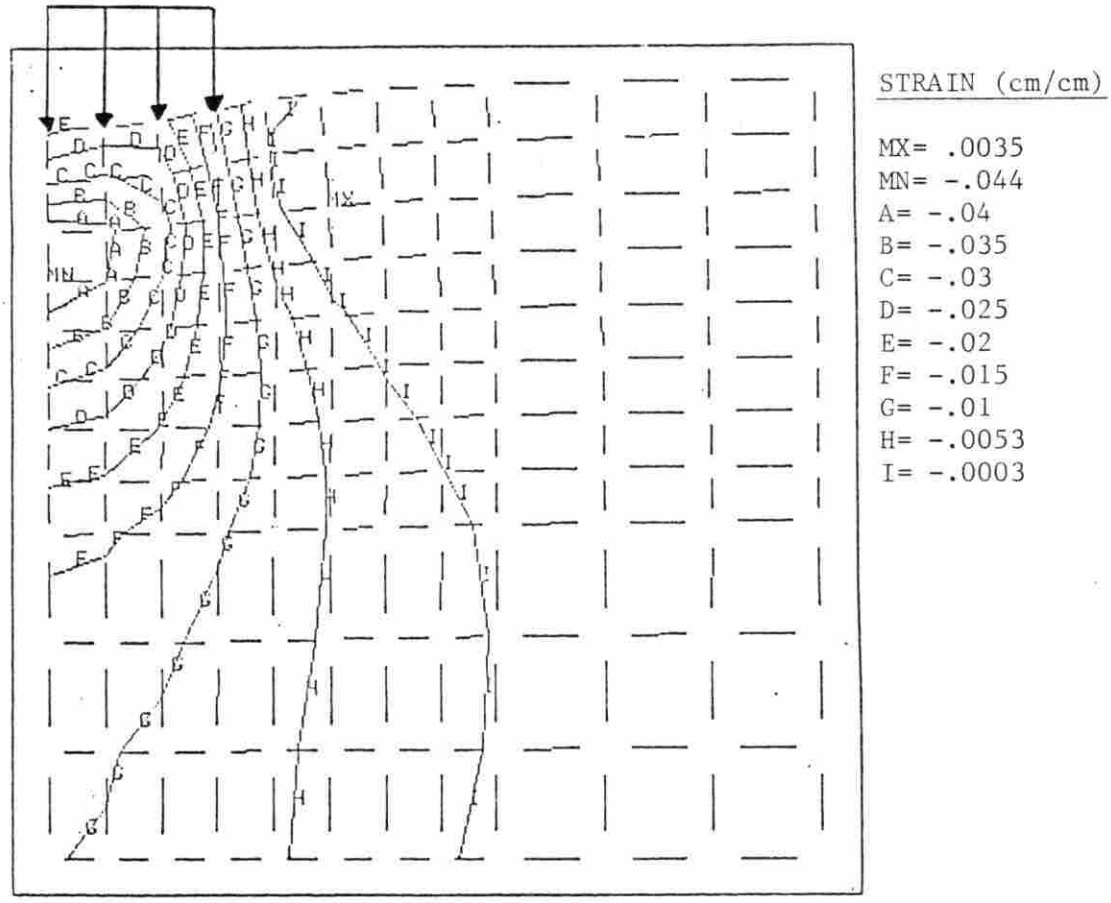

Figure 26. Plastic vertical-strain contours for the uniform low strength soil. Pressure for IH 2+2 Bias (treatment 3, Table 1) of 103.4 kPa applied along three elements. The values for the strain contours and the maximum positive (MX) and maximum negative (MN) strains are listed on the right

Table 7. Predicted bulk densities for the uniform soils

Depth	Predicted Bulk Densities			
	high strength	diff[a]	low strength	diff[a]
cm	Mg/m^3	%	Mg/m^3	%
0-15	1.44	0.7	1.19	4.39
15-31	1.44	0.7	1.18	3.51
31-46	1.44	0.7	1.17	2.63
46-61	1.44	0.7	1.16	1.75

[a]Percent difference between the original bulk density and the predicted bulk density after compaction, based on the original bulk density.

experienced by the low strength soil in response to the load of the IH 2+2 Bias (treatment 3).

SUMMARY

The finite element model predictions were not consistent with the measured values for the top layer of a layered soil. The model predicted that the majority of strain that occurred in the top soil layer was elastic. The predicted plastic strain was less than that measured. Comparison of the predicted bulk densities with the measured bulk densities on the basis of total strain (elastic and plastic strain combined), showed that the model under predicted the amount of compaction in the top soil layer, even for the highest simulated vehicle pressure. The predicted bulk densities compared reasonably well with the measured bulk densities for the remaining three soil layers.

The lack of plastic strain predicted by the model could indicate that the nonlinear theory employed in ANSYS is inadequate for modeling soils. Problems were also encountered in determining the stress-strain relationships of the undisturbed soil samples, due to the large amount of variability that was present among samples. It is possible that the modulus of elasticity determined for the upper soil layer was too high.

The model predictions indicate that higher vehicle contact pressures result in greater levels of strain. Some of the strain contours indicated that the maximum horizontal and vertical strains occurred at some finite depth below the soil surface. However, the maximum bulk density increase always occurred in the upper soil layer. The model results indicate that other factors such as total

load, slip, and tractive device vibration need to be considered in simulating the vehicle loads.

The model demonstrates the capability of the finite element method for modeling soil with layered or uniform properties. The strain contours predicted for the uniform soils penetrated to a deeper depth than those predicted for the layered soils.

The following conclusions can be made from this research:

1. The finite element model developed in ANSYS does not accurately predict soil compaction in the upper soil layer for either TTTs or WTTs.
2. The model predicted that the greatest compaction occured in the upper soil layer for all of the simulated vehicle pressures.
3. The model demonstrates that the resulting strain from an applied load is distributed differently for a uniform soil profile compared to a layered soil.
4. The results indicate that more accurate measurement of the soil properties and more accurate simulation of vehicle loading is required in order to accurately predict compaction due to vehicle loading.
5. The ANSYS nonlinear theory may be inadequate for modeling the soil compaction due to TTTs and WTTs.

REFERENCES

Alekseeva, T. V., Artem'ev, K. A., Bromberg, A. A., Voitsekhouskii, and N. A. Ul'yanov. 1972. Trans. 1982. Machines for earthmoving work. Mashinostroenie Publishers, Moscow. Published for U. S. Dept. of Agric. and National Science Foundation, Washington, D. C. Amerind Publishing Co. Pvt. Ltd., New Delhi. Available from the U. S. Department of Commerce, National Technical Information Service, Springfield, VA.

Bekker, M. G. 1956. Theory of land locomation. The University of Michigan Press, Ann Arbor, Michigan.

Blackwell, P. S. and B. D. Soane. 1981. A method of predicting bulk density changes in field soils resulting from compaction by agricultural traffic. J. Soil Sci. 32:51-65.

Blake, G. R., W. W. Nelson, and R. R. Allmaras. 1976. Persistance of subsoil compaction in a mollisol. Soil Sci. Soc. Am. J. 40:943-948.

Bowen, H. D., Hamid J., and P. D. Ayers. 1984. An application of boussinesq's equation to soil dynamics. Paper No. 84-1049. ASAE, St. Joseph, Michigan.

Brixius, W. W. and F. M. Zoz. 1976. Tires and tracks in agriculture. Trans. SAE 85(3):2034-2044.

Burger, J. A., J. U. Perumpral, J. A. Torbert, R. E. Kreh, and S. Minaez. 1983. The effect of track and rubber-tired vehicles on soil compaction. Paper No. 83-1621. ASAE, St. Joseph, Michigan.

Carpenter, Thomas G. and Norman R. Fausey. 1983. Tire subsizing for minimizing subsoil compaction. Paper No. 83-1058. ASAE, St. Joseph, Michigan.

Chancellor, W. J., R. H. Schmidt, and W. H. Soehne. 1962. Laboratory measurement of soil compaction and plastic flow. Trans. ASAE 5(2):235-239.

Desalvo, G. J. and J. A. Swanson. 1985. ANSYS engineering system user's manual. Swanson Analysis Systems, Houston, Pennsylvania.

Gameda, S., Raghaven, G. S. V., Theriault, R., and E. McKyes. 1984. High axle load compaction effect on stresses and subsoil density. Paper No. 84-1547. ASAE, St. Joseph, Michigan.

Gaultney, L., G. W. Krutz, G. C. Stenhardt, and J. B. Liljedahl. 1982. Effects of subsoil compaction on corn yields. Trans. ASAE 25(3):563-569,574.

Janzen, D. C., R. E. Hefner, and D. C. Erbach. 1985. Soil and corn response to track and wheel compaction. Proc. International Conference on Soil Dynamics 5:1023-1038. National Soil Dynamics Laboratory, Auburn, AL.

Johnson, C. E., A. C. Bailey, T. A. Nichols, and R. D. Grisso. 1984. Soil behavior under repeated hydrostatic loading. Paper No. 84-1548. ASAE, St. Joseph, Michigan.

Kogure, K. and N. Sugiyama. 1975. A study of soil thrust exerted by a tracked vehicle. J. Terramechanics 12(3/4):225-238.

Oida, A. 1984. Analysis of rheological deformation of soil by means of finite element method. J. Terramechanics 21(3):237-254.

Perumpral, J. V., J. B. Liljedahl, and W. H. Perloff. 1971. The finite element method for predicting stress distribution and soil deformation under a tractive device. Trans. ASAE 14(6): 1184-1188.

Plackett, C. W. 1984. The ground pressure of some agricultural tyres at low load and with zero sinkage. J. Agric. Engng. Res. 29(2):159-166.

Pollock, D. Jr., J. V. Perumpral, and T. Kuppusamy. 1984. Multipass effects of vehicles on soil compaction. Paper No. 84-1054. ASAE, St. Joseph, Michigan.

Porterfield, J. W. and T. G. Carpenter. 1985. Potential compaction index for agricultural tires. Paper No. 85-1550. ASAE, St. Joseph, Michigan.

Raper, R. L. and D. C. Erbach. 1985. Core sampler evaluation using finite element method. Paper No. 85-1037. ASAE, St. Joseph, Michigan.

Reaves, C. A. and A. W. Cooper. 1960. Stress distribution in soils under tractor loads. Agricultural Engineering 41(1):20-21,31.

Schuler, R. T. and B. Lowery. 1984. Subsoil compaction effect on corn production with two soil types. Paper 84-1032. ASAE, St. Joseph, Michigan.

Soane, B. D. 1973. Techniques for measuring changes in the packing state and cone resistance of soil after the passage of wheels and tracks. J. Soil Sci. 24(3):311-321.

Soehne, Walter. 1958. Fundamentals of distribution and soil compaction under tractor tires. Agricultural Engineering 39(5):276-282.

Spangler, Merlin G. and Richard L. Handy. 1982. Soil engineering. Harper and Row, Publishers, New York, New York.

Stone, J. A. and W. E. Larson. 1980. Rebound of five one-dimensionally compressed unsaturated granular soils. Soil Sci. of Am. J. 44(4):819-822.

Taylor, J. H. 1985. Wheels and tracks - compaction and traction efficiency. Soil Compaction Conference Abstracts and Previews, Compiled by Randall C. Reeder. The Ohio State University, Columbus, Ohio.

Taylor, J. H. and E. C. Burt. 1975. Track and tire performance in agricultural soils. Trans. ASAE 18(4):3-6.

Taylor, James H., Eddie C. Burt, and Alvin C. Baily. 1980. Effect of total load on subsurface soil compaction. Trans. ASAE 23(3):568-570.

Turner, John L. 1984. A semiempirical mobility model for tracked vehicles. Trans. ASAE 27(4):990-996.

Yong, R. N. and E. A. Fattah. 1976. Prediction of wheel-soil interaction and performance using the finite element method. J. Terramechanics 13(4):227-240.

Yong, R. N., E. A. Fattah, and P. Booninsuk. 1978. Analysis and prediction of tyre-soil interaction and performance using finite elements. J. Terramechanics 15(1):43-63.

Vandenberg, G. E. and W. R. Gill. 1962. Pressure distribution between a smooth tire and soil. Trans. ASAE 5(2):105-107.

Voorhees, W. B. 1977. Soil compaction: how it influences moisture, temperature, yield, root growth. Crops Soils 29(6):7-10.

Wittsell, L. E. and J. A. Hobbs. 1965. Soil compaction effects on field plant growth. Agronomy Journal 57:534-537.

Wong, J. V. 1978. Theory of ground vehicles. John Wiley & Sons, New York, New York.

ACKNOWLEDGEMENTS

A project such as this one could not be completed without the help of others. I'd like to thank the following people who helped in a variety of ways:

To the Lord, for giving me life and the strength to carry out this particular project.

To Dr. Donald Erbach, my major professor, for providing leadership and direction throughout my research.

To Dr. Steve Marley and Dr. Jeff Huston for serving as committee members.

To Randy Raper, Chang Choi, and Mary Anne Dixon, fellow graduate students who lent a helping hand in a variety of ways.

To Bob Fish, Rich Vandepol, Jeff Erb, and Orville Rutzen for their time and assistance in collecting soil samples and machining the steel sampling rings.

To Dr. Faoud Fanous for his help in interpreting and working with the nonlinear aspects of ANSYS.

To Mike Carley for his assistance in working with SAS.

To Scott Farris and Doug Luzbetak for their help and assistance.

To my parents, for their continual support throughout my entire life.

To Brigitte, who has made the last few months much more enjoyable.

APPENDIX A. LAYOUT OF SOIL COMPACTION EXPERIMENT FIELD PLOTS AND INDIVIDUAL PLOT LAYOUT

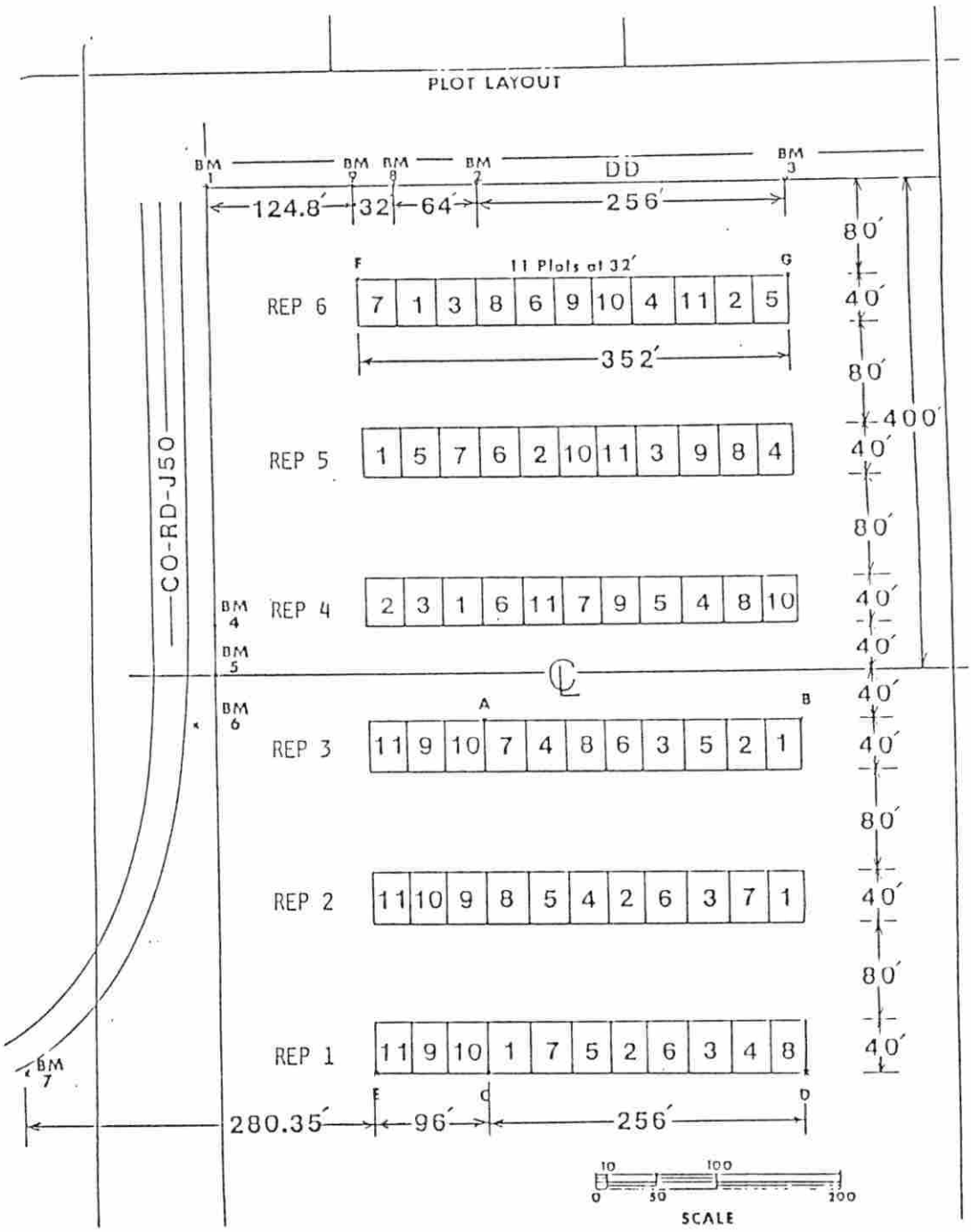

Figure A.1 Layout of compaction field plots

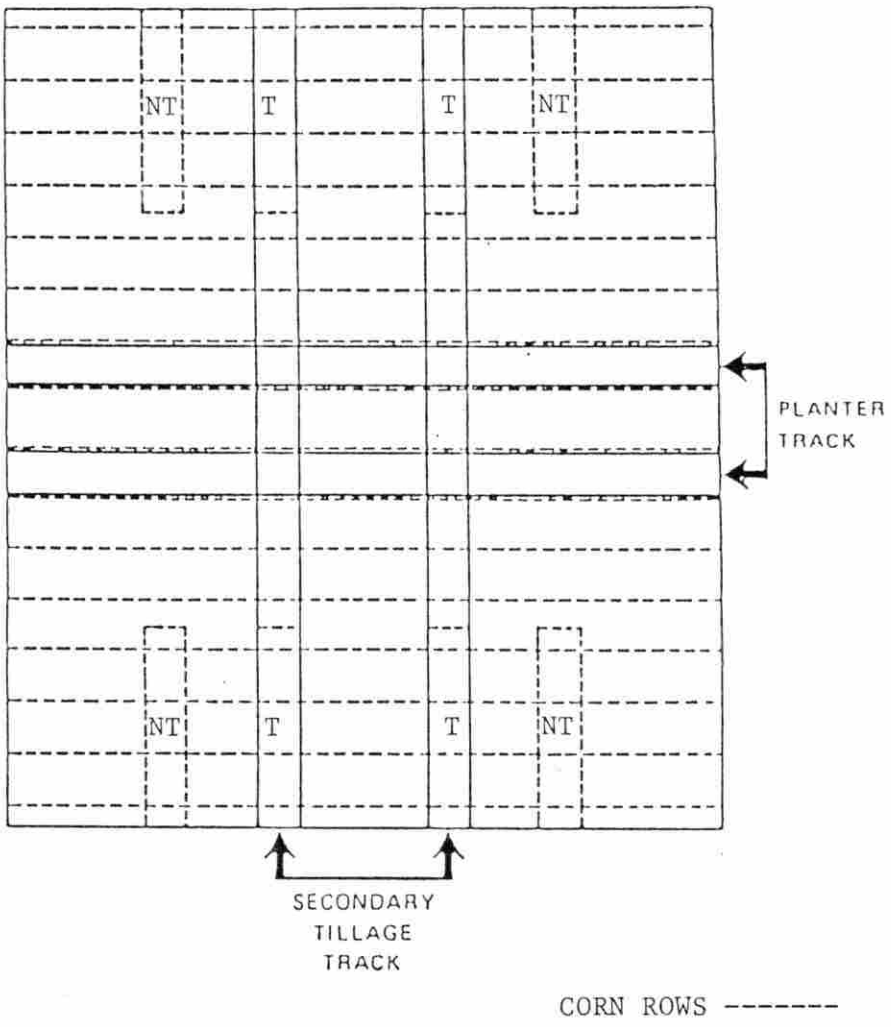

Figure A.2 Individual plot layout. T and NT denote the subplots from which the soil properties and plant measurements are determined for the trafficked and untrafficked soil, respectively

APPENDIX B. EXAMPLE FINITE ELEMENT PROGRAM DEVELOPED IN ANSYS

```
*****************************************************************
* EXAMPLE FINITE ELEMENT PROGRAM DEVELOPED IN ANSYS FOR MODELING    *
* SOIL COMPACTION BY P. W. GASSMAN                                  *
*****************************************************************
*
***ACCESS ANSYS PREPROCESSING***
/INTER,NO
/PREP7
*
***DECLARE STATIC ANALYSIS***
KAN,0
*
***DECLARE NONLINEAR ANALYSIS***
KNL,1
*
***CHOOSE LARGE DISPLACEMENT OPTION***
KAY,6,1
*
***DECLARE ELEMENT TYPE AND ELEMENT KEYOPTS***
ET,1,42,0,0,2,0,0,0
*
***INPUT THE NODAL VALUES IN cm***
N,1,0,0
N,9,60.96,0
FILL
N,97,0,-60.96
N,105,60.96,-60.96
FILL
FILL,1,97,7,,,9,1,1
N,12,106.68,0
N,108,106.68,-60.96
FILL,12,108,7,24,12
FILL,9,12,2,10,1,9,12,1
N,133,0,-106.68
N,141,60.96,-106.68
FILL
FILL,97,133,2,109,12,9,1,1
N,118,76.2,-76.2
N,120,106.68,-76.2
FILL
N,130,76.2,-91.44
N,132,106.68,-91.44
FILL,142,76.2,-106.68
N,144,106.68,-106.68
FILL
*
***PRODUCE ELEMENT MESH***
E,13,14,2,1
EGEN,11,1,1,1,1
EGEN,11,12,1,11,1
```

```
*
***CONSTRAIN VERTICAL BOUNDARIES FOR ZERO HORIZONTAL DISPLACEMENT***
D,1,UX,0.0,,133,12
D,12,UX,0.0,,144,12
*
***CONSTRAIN LOWER HORZ. BOUNDARY FOR ZERO VERTICAL DISPLACEMENT***
D,133,UY,0.0,,144,1
*
***SET NUMBER OF ITERATIONS AND DATA WRITE CONTROLS***
ITER,-5,5,5
POSTR,5,1,5
*
***SET CONVERGENCE CRITERIA***
CNVR,0.01,0.1,0.001
*
***INPUT VALUE FOR ACCELARATION OF GRAVITY (cm/s2)
ACCEL,0.0,981.0,0.0
*
***INPUT LOADS IN dy/cm2 FOR TREATMENT 3 (IH 2+2 BIAS) IN ONE***
***LOAD STEP ACROSS THREE ELEMENTS***
P,1,2,1034483
P,2,3,1034483
P,3,4,1034483
*
***INPUT MATERIAL PROPERTIES FOR MODULUS OF ELASTICITY (dy/cm2),***
***BULK DENSITY (gm/cm3), & POISSON'S RATIO FOR A UNIFORM SOIL***
***(LAYER 1 OF TREATMENT 3 SOIL DATA) OVER TEMPERATURE RANGE FROM***
***0 TO 2300 (MATERIAL PROPERTIES NOT DEPENDENT ON TEMPERATURE)***
MPTEMP,1,0.0,2300,0.0
MPDATA,EX,1,1,38674000,38674000,0
MPDATA,DENS,1,1,1.12,1.12,0
MPDATA,NUXY,1,1,0.4,0.4,0
*
***INPUT NONLINEAR DATA FOR LAYER 1 OF TREATMENT 3 SOIL DATA***
***ELASTIC-PLASTIC OPTION 17 (MULTILINEAR KINEMATIC HARDENING)***
***SPECIFIED***
NL,1,1,0.0,0.0,0.0,0.0
NL,1,5,0.0,0.0,0.0,0.0
NL,1,9,0.0,0.0,0.0,0.0
NL,1,13,17,0.0025,0.009,0.02
NL,1,17,0.07,0.26,0.0,96686
NL,1,21,193371,290057,580114,1933712
NL,1,25,100.0,96686,193371,290057
NL,1,29,580114,1933712,0.0,0.0
NL,1,33,0.0,0.0,0.0,0.0
NL,1,37,0.0,0.0,0.0,0.0
NL,1,41,0.0,0.0,0.0,0.0
NL,1,45,0.0,0.0,0.0,0.0
*
***WRITE DATA TO FILE27 FOR EXECUTION***
```

```
AFWRITE
*
FINISH
*
***BEGIN EXECUTION***
/OUTPUT,BIAS1,DAT
/EXE
/INPUT,27
*
***POSTPROCESSING IN POST1***
/INTER,NO
/POST1
*
***CALL UP STORED STRAIN VALUES FROM FILE12***
STRESS,ELX,42,78
STRESS,ELY,42,79
STRESS,EXY,42,80
STRESS,PLX,42,82
STRESS,PLY,42,83
STRESS,PXY,42,84
*
***USE DATA FROM LOAD STEP 1, ITERATION 5***
SET,1,5
*
***OBTAIN STRAIN PLOTS***
PLNSTR,ELX
PLNSTR,ELY
PLNSTR,EXY
PLNSTR,PLX
PLNSTR,PLY
PLNSTR,PXY
*
FINISH
/EOF
*
***TO CHANGE MATERIAL TYPE IN PREP7***
/INTER,NO
/PREP7
RESUME
*
***DECLARE MATERIAL TYPE 2. MATERIAL PROPERTIES AND NONLINEAR***
***DATA MUST BE INPUT FOR EACH MATERIAL TYPE***
MAT,2
*
***CHANGE ALL ELEMENTS TO MATERIAL TYPE 2***
ERSEL,ELEM,1,121
EMODIF,ALL,0
*
***RESTORE ALL ELEMENTS FOR PROCESSING***
EALL
```

APPENDIX C. PROGRAM AND DATA USED TO DETERMINE BULK DENSITY AND MOISTURE CONTENT VALUES FOR SOIL LAYERS

```
*****************************************************************
*SAS PROGRAM FOR CALCULATING BULK DENSITY AND MOISTURE CONTENT*
*****************************************************************
DATA;
INPUT FIELD REP TRT DEP CAN WW DW TW;
WW=WW/10;
DW=DW/10;
TW=TW/10;
DEP = 2.5 + (DEP - 1) * 5.0;
MOIST=100*(WW-DW)/(DW-TW);
BULKD=(DW-TW)/228;
MMH20=(MOIST/100)*BULKD*50;
CARDS;
***DATA GOES HERE***
PROC SORT;
   BY REP TRT WHL LAYER;
PROC MEANS;
   BY REP TRT WHL LAYER;
   VAR BULKD;
   OUTPUT OUT=LAYBD MEAN=MBULK;
PROC SORT DATA=LAYBD;
   BY WHL LAYER;
PROC MEANS DATA=LAYBD;
   BY WHL LAYER;
   VAR MBULK;
```

EXPERIMENTAL DATA DETERMINED FROM FIELD TESTS USED TO CALCULATE DRY BULK DENSITY AND MOISTURE CONTENT:

TRT: 4 - 855 BELT
5 - IH 2+2 BIAS
6 - IH 2+2 TERRA
11 - MPSPL STEEL

TRACK: 1 - UNTRAFFICKED
2 - TRAFFICKED

DEPTH: 1; 0-5.08 cm
2; 5.08-10.16 cm
3; 10.16-15.24 cm
4; 15.24-20.32 cm
5; 20.32-25.40 cm
6; 25.40-30.48 cm
7; 30.48-35.56 cm
8; 35.56-40.64 cm
9; 40.64-45.72 cm
10; 45.72-50.80 cm
11; 50.80-55.88 cm
12; 55.88-60.96 cm
13; 60.96-66.04 cm

FIELD	REP	TRT	TRACK	DEPTH	CAN	WET WT	DRY WT	TARE WT
						---------gm*10---------		
60186	1	11	1	1	1	2898	3358	753
60186	1	11	1	2	2	4403	3581	748
60186	1	11	1	3	3	4549	3695	764

60186	1	11	1	4	4	5428	4296	761
60186	1	11	1	5	5	5479	4551	731
60186	1	11	1	6	6	5365	4462	740
60186	1	11	1	7	7	5292	4408	752
60186	1	11	1	8	8	5385	4514	755
60186	1	11	1	9	9	5282	4476	754
60186	1	11	1	10	10	5297	4476	757
60186	1	11	1	11	11	5298	4462	750
60186	1	11	1	12	12	5446	4549	765
60186	1	11	1	13	13	5124	4262	754
60186	1	11	2	1	14	3414	2972	757
60186	1	11	2	2	15	4076	3333	727
60186	1	11	2	3	16	4968	4008	756
60186	1	11	2	4	17	4643	3743	750
60186	1	11	2	5	18	4869	3948	751
60186	1	11	2	6	19	5068	4213	756
60186	1	11	2	7	20	5170	4296	747
60186	1	11	2	8	21	5261	4378	758
60186	1	11	2	9	22	5120	4226	755
60186	1	11	2	10	23	5215	4373	753
60186	1	11	2	11	24	5121	4285	750
60186	1	11	2	12	25	5413	4515	752
60186	1	11	2	13	26	5284	4391	750
60186	1	5	1	1	131	3456	3040	743
60186	1	5	1	2	132	4031	3376	741
60186	1	5	1	3	133	4781	4002	731
60186	1	5	1	4	134	5002	4187	732
60186	1	5	1	5	135	4875	4084	755
60186	1	5	1	6	136	4794	4055	752
60186	1	5	1	7	137	5052	4275	756
60186	1	5	1	8	138	5353	4568	745
60186	1	5	1	9	139	5446	4640	756
60186	1	5	1	10	140	5142	4407	746
60186	1	5	1	11	141	5348	4551	752
60186	1	5	1	12	142	5253	4552	745
60186	1	5	1	13	143	5624	4790	758
60186	1	5	2	1	144	3498	3031	748
60186	1	5	2	2	145	4413	3718	736
60186	1	5	2	3	146	5183	4303	737
60186	1	5	2	4	147	4832	3974	755
60186	1	5	2	5	148	5128	4283	733
60186	1	5	2	6	149	5139	4301	755
60186	1	5	2	7	150	5326	4507	735
60186	1	5	2	8	151	5197	4409	744
60186	1	5	2	9	152	5471	4638	752
60186	1	5	2	10	153	5350	4578	763
60186	1	5	2	11	154	5140	4377	763
60186	1	5	2	12	155	5295	4478	742
60186	1	5	2	13	156	5295	4466	730
60186	1	6	1	1	183	3714	3333	759

60186	1	6	1	2	184	4000	3436	742
60186	1	6	1	3	185	4608	3918	747
60186	1	6	1	4	186	4986	4247	771
60186	1	6	1	5	187	4789	4054	741
60186	1	6	1	6	188	5101	4355	745
60186	1	6	1	7	189	5577	4788	750
60186	1	6	1	8	190	5345	4580	744
60186	1	6	1	9	191	5161	4366	756
60186	1	6	1	10	192	5576	4780	750
60186	1	6	1	11	193	5286	4496	750
60186	1	6	1	12	194	5397	4590	736
60186	1	6	1	13	195	5264	4457	754
60186	1	6	2	1	196	3531	3161	733
60186	1	6	2	2	197	4622	3921	745
60186	1	6	2	3	198	4991	4206	750
60186	1	6	2	4	199	5049	4267	743
60186	1	6	2	5	200	4873	4102	745
60186	1	6	2	6	201	5033	4311	755
60186	1	6	2	7	202	5469	4716	745
60186	1	6	2	8	203	5346	4620	742
60186	1	6	2	9	204	5216	4489	742
60186	1	6	2	10	205	5157	4443	743
60186	1	6	2	11	206	5480	4697	736
60186	1	6	2	12	207	5225	4505	753
60186	1	6	2	13	208	5275	4531	748
60186	1	4	1	1	235	3511	3163	751
60186	1	4	1	2	236	4678	3515	753
60186	1	4	1	3	237	4632	3946	754
60186	1	4	1	4	238	4742	4033	747
60186	1	4	1	5	239	5101	4322	745
60186	1	4	1	6	240	5435	4705	750
60186	1	4	1	7	241	5425	4681	730
60186	1	4	1	8	242	5651	4917	748
60186	1	4	1	9	243	5374	4661	754
60186	1	4	1	10	244	5538	4807	746
60186	1	4	1	11	245	5134	4445	754
60186	1	4	1	12	246	5328	4596	741
60186	1	4	1	13	247	5336	4568	748
60186	1	4	2	1	248	3554	3185	738
60186	1	4	2	2	249	4666	4004	760
60186	1	4	2	3	250	5124	4347	745
60186	1	4	2	4	251	5086	4287	744
60186	1	4	2	5	252	5184	4400	752
60186	1	4	2	6	253	5367	4626	738
60186	1	4	2	7	254	5482	4730	771
60186	1	4	2	8	255	5364	4659	763
60186	1	4	2	9	256	5244	4501	755
60186	1	4	2	10	257	5279	4586	763
60186	1	4	2	11	258	5358	4643	741
60186	1	4	2	12	259	5449	4679	758

60186	1	4	2	13	260	5370	4597	747
60186	2	11	1	1	313	2937	2609	757
60186	2	11	1	2	314	4106	3327	746
60186	2	11	1	3	315	4542	3689	747
60186	2	11	1	4	316	4748	3814	730
60186	2	11	1	5	317	5959	4069	760
60186	2	11	1	6	318	5326	4340	722
60186	2	11	1	7	319	5044	4113	741
60186	2	11	1	8	320	4993	4071	753
60186	2	11	1	9	321	5325	4320	739
60186	2	11	1	10	322	5064	4126	742
60186	2	11	1	11	323	5099	4135	752
60186	2	11	1	12	324	5310	4293	751
60186	2	11	1	13	325	5209	4222	745
60186	2	11	2	1	326	2849	2477	764
60186	2	11	2	2	327	4066	3244	750
60186	2	11	2	3	328	4938	4035	752
60186	2	11	2	4	329	4597	3704	726
60186	2	11	2	5	330	4956	4033	765
60186	2	11	2	6	331	4999	4044	747
60186	2	11	2	7	332	5140	4164	737
60186	2	11	2	8	333	4952	4013	750
60186	2	11	2	9	334	5169	4182	750
60186	2	11	2	10	335	5060	4087	741
60186	2	11	2	11	336	4994	4021	767
60186	2	11	2	12	337	5062	4065	746
60186	2	11	2	13	338	5351	4287	721
60186	2	5	1	1	417	2733	2437	739
60186	2	5	1	2	418	4051	3384	752
60186	2	5	1	3	419	5024	4174	760
60186	2	5	1	4	420	4758	3938	754
60186	2	5	1	5	421	5029	4174	757
60186	2	5	1	6	422	5518	4665	764
60186	2	5	1	7	423	5350	4550	762
60186	2	5	1	8	424	5351	4542	760
60186	2	5	1	9	425	5203	4395	739
60186	2	5	1	10	426	5366	4524	744
60186	2	5	1	11	427	5337	4493	748
60186	2	5	1	12	428	5337	4489	750
60186	2	5	1	13	429	5397	4511	740
60186	2	5	2	1	430	2740	2429	755
60186	2	5	2	2	431	4902	4037	755
60186	2	5	2	3	432	4986	4118	722
60186	2	5	2	4	433	5405	4475	756
60186	2	5	2	5	434	5273	4395	755
60186	2	5	2	6	435	5127	4318	754
60186	2	5	2	7	436	5304	4494	739
60186	2	5	2	8	437	5311	4491	745
60186	2	5	2	9	438	5266	4425	758
60186	2	5	2	10	439	5145	4335	751

60186	2	5	2	11	440	5270	4415	733
60186	2	5	2	12	441	5231	4382	744
60186	2	5	2	13	442	5089	4260	753
60186	2	4	1	1	443	2590	2322	738
60186	2	4	1	2	444	3583	2878	749
60186	2	4	1	3	445	4817	3864	765
60186	2	4	1	4	446	4884	3974	752
60186	2	4	1	5	447	5070	4156	739
60186	2	4	1	6	448	5232	4285	757
60186	2	4	1	7	449	5076	4138	737
60186	2	4	1	8	450	5267	4295	755
60186	2	4	1	9	451	5260	4268	745
60186	2	4	1	10	452	5210	4242	749
60186	2	4	1	11	453	5069	4125	736
60186	2	4	1	12	454	5259	4265	751
60186	2	4	1	13	455	5266	4290	759
60186	2	4	2	1	456	4029	3368	769
60186	2	4	2	2	457	4900	3963	762
60186	2	4	2	3	458	5049	4093	771
60186	2	4	2	4	459	4971	4035	747
60186	2	4	2	5	460	4992	3996	733
60186	2	4	2	6	461	5028	4032	735
60186	2	4	2	7	462	4977	3995	752
60186	2	4	2	8	463	5022	4032	745
60186	2	4	2	9	464	5096	4089	751
60186	2	4	2	10	465	4927	3938	740
60186	2	4	2	11	466	5119	4099	744
60186	2	4	2	12	467	4909	3918	752
60186	2	4	2	13	468	4926	3931	741
60186	2	6	1	1	495	2873	2598	752
60186	2	6	1	2	496	4143	3497	757
60186	2	6	1	3	497	4845	4056	768
60186	2	6	1	4	498	4783	3993	759
60186	2	6	1	5	499	4916	4140	739
60186	2	6	1	6	500	5307	4519	748
60186	2	6	1	7	501	5246	4462	747
60186	2	6	1	8	502	5330	4531	750
60186	2	6	1	9	503	5319	4517	753
60186	2	6	1	10	504	5274	4486	740
60186	2	6	1	11	505	5347	4528	753
60186	2	6	1	12	506	5465	4608	752
60186	2	6	1	13	507	5329	4493	749
60186	2	6	2	1	508	2648	2419	751
60186	2	6	2	2	509	4795	4017	754
60186	2	6	2	3	510	49c7	4153	744
60186	2	6	2	4	511	5091	4281	754
60186	2	6	2	5	512	5120	4308	751
60186	2	6	2	6	513	5159	4377	758
60186	2	6	2	7	514	5186	4449	753
60186	2	6	2	8	515	5344	4574	752

60186	2	6	2	9	516	5209	4460	766
60186	2	6	2	10	517	5271	4501	752
60186	2	6	2	11	518	5332	4514	764
60186	2	6	2	12	519	5343	4549	762
60186	2	6	2	13	520	5384	4568	727
60186	3	11	1	1	625	2838	2542	756
60186	3	11	1	2	626	4207	3472	747
60186	3	11	1	3	627	4230	3402	768
60186	3	11	1	4	628	4730	3872	765
60186	3	11	1	5	629	5300	4368	743
60186	3	11	1	6	630	5293	4387	762
60186	3	11	1	7	631	5330	4416	736
60186	3	11	1	8	632	5122	4205	737
60186	3	11	1	9	633	5094	4172	732
60186	3	11	1	10	634	5162	4216	765
60186	3	11	1	11	635	5275	4295	754
60186	3	11	1	12	636	4990	4047	743
60186	3	11	1	13	637	5321	4297	738
60186	3	11	2	1	638	3586	3105	735
60186	3	11	2	2	639	4764	3877	761
60186	3	11	2	3	640	4693	3816	737
60186	3	11	2	4	641	4819	3934	743
60186	3	11	2	5	642	5222	4327	755
60186	3	11	2	6	643	5033	4154	760
60186	3	11	2	7	644	5170	4246	753
60186	3	11	2	8	645	5347	4382	750
60186	3	11	2	9	646	5010	4110	736
60186	3	11	2	10	647	5187	4250	743
60186	3	11	2	11	648	5068	4130	749
60186	3	11	2	12	649	5106	4156	770
60186	3	11	2	13	650	5105	4163	768
60186	3	4	1	1	729	3482	3139	758
60186	3	4	1	2	730	4344	3670	745
60186	3	4	1	3	731	4508	3792	755
60186	3	4	1	4	732	4772	4016	741
60186	3	4	1	5	733	5183	4432	758
60186	3	4	1	6	734	5364	4591	745
60186	3	4	1	7	735	5157	4405	752
60186	3	4	1	8	736	5337	4548	751
60186	3	4	1	9	737	5148	4394	736
60186	3	4	1	10	738	5337	4557	742
60186	3	4	1	11	739	5385	4586	765
60186	3	4	1	12	740	5175	4388	750
60186	3	4	1	13	741	5342	4517	770
60186	3	4	2	1	742	3693	3257	741
60186	3	4	2	2	743	4822	4045	740
60186	3	4	2	3	744	4992	4184	759
60186	3	4	2	4	745	5049	4255	742
60186	3	4	2	5	746	5123	4355	734
60186	3	4	2	6	747	5311	4571	768

60186	3	4	2	7	748	5291	4512	743
60186	3	4	2	8	749	5321	4518	770
60186	3	4	2	9	750	5172	4392	757
60186	3	4	2	10	751	5260	4474	768
60186	3	4	2	11	752	5147	4362	741
60186	3	4	2	12	753	5301	4474	756
60186	3	4	2	13	754	5104	4303	756
60186	3	6	1	1	781	3454	3026	759
60186	3	6	1	2	782	4544	3777	754
60186	3	6	1	3	783	4938	4077	756
60186	3	6	1	4	784	4957	4072	753
60186	3	6	1	5	785	5204	4359	759
60186	3	6	1	6	786	5391	4604	751
60186	3	6	1	7	787	5343	4544	754
60186	3	6	1	8	788	5377	4562	751
60186	3	6	1	9	789	5148	4372	740
60186	3	6	1	10	790	5349	4540	757
60186	3	6	1	11	791	5322	4522	761
60186	3	6	1	12	792	5458	4624	757
60186	3	6	1	13	793	5442	4621	740
60186	3	6	2	1	794	4150	3612	766
60186	3	6	2	2	795	4640	4107	759
60186	3	6	2	3	796	4974	4105	738
60186	3	6	2	4	797	5161	4291	750
60186	3	6	2	5	798	5224	4381	750
60186	3	6	2	6	799	5454	4630	743
60186	3	6	2	7	800	5300	4533	757
60186	3	6	2	8	801	5411	4623	767
60186	3	6	2	9	802	5218	4468	740
60186	3	6	2	10	803	5414	4626	745
60186	3	6	2	11	804	5212	4444	727
60186	3	6	2	12	805	5468	4645	744
60186	3	6	2	13	806	5433	4614	754
60186	3	5	1	1	833	2755	2490	754
60186	3	5	1	2	834	3986	3330	760
60186	3	5	1	3	835	4124	3431	746
60186	3	5	1	4	836	4615	3791	737
60186	3	5	1	5	837	5265	4327	767
60186	3	5	1	6	838	5143	4253	760
60186	3	5	1	7	839	5189	4293	764
60186	3	5	1	8	840	5302	4381	753
60186	3	5	1	9	841	5252	4335	760
60186	3	5	1	10	842	5208	4304	751
60186	3	5	1	11	843	5174	4240	751
60186	3	5	1	12	844	5375	4390	761
60186	3	5	1	13	845	5238	4255	780
60186	3	5	2	1	846	3681	3238	749
60186	3	5	2	2	847	4431	3679	757
60186	3	5	2	3	848	4873	3973	760
60186	3	5	2	4	849	4978	4073	732

60186	3	5	2	5	850	5516	4583	739
60186	3	5	2	6	851	5185	4293	756
60186	3	5	2	7	852	5138	4257	755
60186	3	5	2	8	853	5351	4427	765
60186	3	5	2	9	854	5188	4303	754
60186	3	5	2	10	855	5225	4304	765
60186	3	5	2	11	856	5228	4273	741
60186	3	5	2	12	857	5176	4255	752
60186	3	5	2	13	858	5367	4420	753

APPENDIX D. SAS PROGRAM USED TO DETERMINE CONFIDENCE INTERVALS FOR FIGURE 16 AND STRESS-STRAIN DATA DETERMINED FROM UNIVERSAL TESTING MACHINE

```
*********************************************************************
*SAS PROGRAM FOR CALCULATING CONFIDENCE INTERVALS OF ONE STANDARD*
*DEVIATION FOR THE STRESS-STRAIN DATA                               *
*********************************************************************
DATA;
INPUT TRT REP DEPTH STRESS STRAIN;
CARDS;
***INPUT DATA HERE***
PROC SORT;
   BY DEPTH STRESS;
PROC MEANS;
   BY DEPTH STRESS;
   VAR STRAIN;
   OUTPUT OUT=NEW  MEAN=M STD=S;
DATA NEW;
   SET NEW;
   MUP=M+S;
   MDN=M-S;
DATA A;
   SET NEW;
   X=MUP;
   KEEP STRESS DEPTH X;
DATA B;
   SET NEW;
   X=MDN;
   KEEP STRESS DEPTH X;
PROC SORT DATA=B;
   BY DESCENDING STRESS;
DATA FINAL;
   SET A B;
PROC SORT DATA=FINAL;
   BY DEPTH;
TITLE .C=BLACK .H=2 .F=TRIPLEX CONFIDENCE INTERVALS FOR;
TITLE2 .C=BLACK .H=2 .F=TRIPLEX ONE STANDARD DEVIATION;
LABEL STRESS=STRESS/kPa/ X=STRAIN (cm/cm);
PROC GPLOT DATA=FINAL;
   PLOT STRESS * X=DEPTH/HAXIS=-.05 TO .30 BY 0.05 VAXIS=0 TO 200
   BY 50;
SYMBOL1 W=1 V=NONE C=BLACK I=M1X;
SYMBOL2 W=1 V=NONE C=BLACK I=M5;
SYMBOL3 W=1 V=NONE C=BLACK I=M1;
SYMBOL4 W=1 V=NONE C=BLACK I=M5X;
```

STRESS-STRAIN DATA DETERMINED FROM UNIVERSAL TESTING MACHINE

TRT: 1 - MPSPL STEEL
2 - 855 BELT
3 - IH 2+2 BIAS
4 - IH 2+2 TERRA

DEPTH: 1; 0-15.24 cm
2; 15.24-30.48 cm
3; 30.48-45.72 cm
4; 45.72-60.96 cm

TRT	REP	DEPTH	STRESS	STRAIN
1	1	1	0.0	.0
1	1	1	9.7	.012
1	1	1	19.3	.018
1	1	1	29.0	.026
1	1	1	38.7	.037
1	1	1	48.3	.052
1	1	1	58.0	.071
1	1	1	67.7	.093
1	1	1	77.3	.110
1	1	1	87.0	.140
1	1	1	96.7	.160
1	1	1	106.4	.190
1	1	1	116.0	.220
1	2	1	0.0	.0
1	2	1	9.7	.016
1	2	1	19.3	.034
1	2	1	29.0	.050
1	2	1	38.7	.062
1	2	1	48.3	.072
1	2	1	58.0	.081
1	2	1	67.7	.090
1	2	1	77.3	.096
1	2	1	87.0	.100
1	2	1	96.7	.110
1	2	1	106.4	.120
1	2	1	116.0	.130
1	1	2	0.0	.0
1	1	2	9.7	.025
1	1	2	19.3	.031
1	1	2	38.7	.039
1	1	2	58.0	.045
1	1	2	67.7	.049
1	1	2	77.3	.052
1	1	2	87.0	.057
1	1	2	96.7	.063
1	1	2	106.4	.070
1	1	2	116.0	.079
1	1	2	135.4	.100
1	1	2	154.7	.130
1	1	2	193.4	.190
1	2	2	9.7	.0023

1	2	2	0.0	.0
1	2	2	19.3	.0038
1	2	2	38.7	.0064
1	2	2	58.0	.01
1	2	2	67.7	.014
1	2	2	77.3	.019
1	2	2	87.0	.027
1	2	2	96.7	.036
1	2	2	106.4	.045
1	2	2	116.0	.057
1	2	2	135.4	.083
1	2	2	154.7	.11
1	2	2	193.4	.17
1	3	2	0.0	.0
1	3	2	9.7	.0026
1	3	2	19.3	.0047
1	3	2	38.7	.0095
1	3	2	58.0	.014
1	3	2	67.7	.016
1	3	2	77.3	.018
1	3	2	87.0	.02
1	3	2	96.7	.023
1	3	2	106.4	.025
1	3	2	116.0	.030
1	3	2	135.4	.041
1	3	2	154.7	.06
1	3	2	193.4	.09
1	1	3	0.0	.0
1	1	3	19.3	.0046
1	1	3	38.7	.0065
1	1	3	58.0	.009
1	1	3	77.3	.01
1	1	3	96.7	.012
1	1	3	116.0	.014
1	1	3	135.4	.016
1	1	3	154.7	.017
1	1	3	193.4	.020
1	2	3	0.0	.0
1	2	3	19.3	.003
1	2	3	38.7	.0045
1	2	3	58.0	.007
1	2	3	77.3	.01
1	2	3	96.7	.013
1	2	3	116.0	.018
1	2	3	135.4	.023
1	2	3	154.7	.029
1	2	3	193.4	.045
1	3	3	0.0	.0
1	3	3	19.3	.003
1	3	3	38.7	.0044

1	3	3	58.0	.006
1	3	3	77.3	.0074
1	3	3	96.7	.009
1	3	3	116.0	.01
1	3	3	135.4	.012
1	3	3	154.7	.013
1	3	3	193.4	.017
1	1	4	0.0	.0
1	1	4	38.7	.01
1	1	4	77.3	.016
1	1	4	116.0	.02
1	1	4	154.7	.025
1	1	4	193.4	.03
1	2	4	0.0	.0
1	2	4	38.7	.006
1	2	4	77.3	.008
1	2	4	116.0	.011
1	2	4	154.7	.013
1	2	4	193.4	.015
1	3	4	0.0	.0
1	3	4	38.7	.005
1	3	4	77.3	.009
1	3	4	116.0	.013
1	3	4	154.7	.019
1	3	4	193.4	.027
2	1	1	0.0	.0
2	1	1	9.7	.004
2	1	1	19.3	.006
2	1	1	29.0	.009
2	1	1	38.7	.012
2	1	1	48.3	.016
2	1	1	58.0	.02
2	1	1	67.7	.028
2	1	1	77.3	.042
2	1	1	87.0	.06
2	1	1	96.7	.081
2	1	1	106.4	.1
2	1	1	116.0	.12
2	1	1	135.4	.15
2	1	1	154.7	.18
2	1	1	193.4	.23
2	2	1	0.0	.0
2	2	1	9.7	.002
2	2	1	19.3	.003
2	2	1	29.0	.0046
2	2	1	38.7	.006
2	2	1	48.3	.0075
2	2	1	58.0	.010
2	2	1	67.7	.013
2	2	1	77.3	.018

2	2	1	87.0	.024
2	2	1	96.7	.033
2	2	1	106.4	.044
2	2	1	116.0	.058
2	2	1	135.4	.086
2	2	1	154.7	.12
2	2	1	193.4	.16
2	1	2	0.0	.0
2	1	2	9.7	.005
2	1	2	19.3	.009
2	1	2	38.7	.014
2	1	2	58.0	.021
2	1	2	67.7	.026
2	1	2	77.3	.033
2	1	2	87.0	.042
2	1	2	96.7	.051
2	1	2	106.4	.06
2	1	2	116.0	.073
2	1	2	135.4	.09
2	1	2	154.7	.11
2	1	2	193.4	.15
2	2	2	0.0	.0
2	2	2	9.7	.002
2	2	2	19.3	.003
2	2	2	38.7	.005
2	2	2	58.0	.008
2	2	2	67.7	.009
2	2	2	77.3	.012
2	2	2	87.0	.015
2	2	2	96.7	.019
2	2	2	106.4	.03
2	2	2	116.0	.031
2	2	2	135.4	.05
2	2	2	154.7	.066
2	2	2	193.4	.11
2	3	2	0.0	.0
2	3	2	9.7	.003
2	3	2	19.3	.005
2	3	2	38.7	.008
2	3	2	58.0	.01
2	3	2	67.7	.012
2	3	2	77.3	.014
2	3	2	87.0	.017
2	3	2	96.7	.021
2	3	2	106.4	.025
2	3	2	116.0	.03
2	3	2	135.4	.04
2	3	2	154.7	.054
2	3	2	193.4	.08
2	1	3	0.0	.0

2	1	3	19.3	.0046
2	1	3	38.7	.006
2	1	3	58.0	.008
2	1	3	77.3	.01
2	1	3	96.7	.012
2	1	3	116.0	.014
2	1	3	135.4	.016
2	1	3	154.7	.02
2	1	3	193.4	.03
2	2	3	0.0	.0
2	2	3	19.3	.003
2	2	3	38.7	.004
2	2	3	58.0	.005
2	2	3	77.3	.006
2	2	3	96.7	.007
2	2	3	116.0	.008
2	2	3	135.4	.009
2	2	3	154.7	.01
2	2	3	193.4	.012
2	3	3	0.0	.0
2	3	3	19.3	.004
2	3	3	38.7	.0065
2	3	3	58.0	.009
2	3	3	77.3	.012
2	3	3	96.7	.017
2	3	3	116.0	.018
2	3	3	135.4	.021
2	3	3	154.7	.024
2	3	3	193.4	.031
2	1	4	0.0	.0
2	1	4	38.7	.006
2	1	4	77.3	.008
2	1	4	116.0	.01
2	1	4	154.7	.014
2	1	4	193.4	.023
2	2	4	0.0	.0
2	2	4	38.7	.0046
2	2	4	77.3	.01
2	2	4	116.0	.017
2	2	4	154.7	.025
2	2	4	193.4	.035
3	1	1	0.0	.0
3	1	1	9.7	.002
3	1	1	19.3	.0034
3	1	1	29.0	.0046
3	1	1	38.7	.006
3	1	1	48.3	.0075
3	1	1	58.0	.01
3	1	1	67.7	.014
3	1	1	77.3	.02

3	1	1	87.0	.031
3	1	1	96.7	.049
3	1	1	106.4	.07
3	1	1	116.0	.091
3	1	1	135.4	.13
3	1	1	154.7	.17
3	1	1	193.4	.22
3	2	1	0.0	.0
3	2	1	9.7	.003
3	2	1	19.3	.015
3	2	1	29.0	.04
3	2	1	38.7	.066
3	2	1	48.3	.092
3	2	1	58.0	.12
3	2	1	67.7	.14
3	2	1	77.3	.15
3	2	1	87.0	.16
3	2	1	96.7	.18
3	2	1	106.4	.19
3	2	1	116.0	.20
3	2	1	135.4	.22
3	2	1	154.7	.24
3	2	1	193.4	.29
3	1	2	0.0	.0
3	1	2	9.7	.002
3	1	2	19.3	.005
3	1	2	38.7	.009
3	1	2	58.0	.013
3	1	2	67.7	.016
3	1	2	77.3	.018
3	1	2	87.0	.021
3	1	2	96.7	.025
3	1	2	106.4	.029
3	1	2	116.0	.033
3	1	2	135.4	.041
3	1	2	154.7	.05
3	1	2	193.4	.07
3	2	2	0.0	.0
3	2	2	9.7	.002
3	2	2	19.3	.005
3	2	2	38.7	.008
3	2	2	58.0	.01
3	2	2	67.7	.012
3	2	2	77.3	.016
3	2	2	87.0	.017
3	2	2	96.7	.021
3	2	2	106.4	.024
3	2	2	116.0	.028
3	2	2	135.4	.038
3	2	2	154.7	.049

3	2	2	193.4	.07
3	1	3	0.0	.0
3	1	3	19.3	.006
3	1	3	38.7	.009
3	1	3	58.0	.012
3	1	3	77.3	.014
3	1	3	96.7	.018
3	1	3	116.0	.021
3	1	3	135.4	.027
3	1	3	154.7	.034
3	1	3	193.4	.054
3	2	3	0.0	.0
3	2	3	19.3	.002
3	2	3	38.7	.003
3	2	3	58.0	.003
3	2	3	77.3	.005
3	2	3	96.7	.006
3	2	3	116.0	.007
3	2	3	135.4	.008
3	2	3	154.7	.009
3	2	3	193.4	.01
3	3	3	0.0	.0
3	3	3	19.3	.0013
3	3	3	38.7	.002
3	3	3	58.0	.003
3	3	3	77.3	.004
3	3	3	96.7	.005
3	3	3	116.0	.006
3	3	3	135.4	.008
3	3	3	154.7	.009
3	3	3	193.4	.012
3	1	4	0.0	.0
3	1	4	38.7	.003
3	1	4	77.3	.005
3	1	4	135.4	.007
3	1	4	154.7	.009
3	1	4	193.4	.012
3	2	4	0.0	.0
3	2	4	38.7	.005
3	2	4	77.3	.009
3	2	4	135.4	.014
3	2	4	154.7	.02
3	2	4	193.4	.03
3	3	4	0.0	.0
3	3	4	38.7	.003
3	3	4	77.3	.005
3	3	4	135.4	.008
3	3	4	154.7	.011
3	3	4	193.4	.018
4	1	1	0.0	.0

4	1	1	9.7	.010
4	1	1	19.3	.015
4	1	1	29.0	.021
4	1	1	38.7	.029
4	1	1	48.3	.037
4	1	1	58.0	.046
4	1	1	67.7	.057
4	1	1	77.3	.07
4	1	1	87.0	.08
4	1	1	96.7	.093
4	1	1	106.4	.11
4	1	1	116.0	.12
4	1	1	135.4	.14
4	1	1	154.7	.16
4	2	1	0.0	.0
4	2	1	9.7	.04
4	2	1	19.3	.066
4	2	1	29.0	.083
4	2	1	38.7	.1
4	2	1	48.3	.11
4	2	1	58.0	.13
4	2	1	67.7	.14
4	2	1	77.3	.16
4	2	1	87.0	.17
4	2	1	96.7	.19
4	2	1	106.4	.21
4	2	1	116.0	.22
4	2	1	135.4	.25
4	2	1	154.7	.28
4	3	1	0.0	.0
4	3	1	9.7	.005
4	3	1	19.3	.009
4	3	1	29.0	.015
4	3	1	38.7	.023
4	3	1	48.3	.031
4	3	1	58.0	.041
4	3	1	67.7	.051
4	3	1	77.3	.061
4	3	1	87.0	.07
4	3	1	96.7	.079
4	3	1	106.4	.086
4	3	1	116.0	.094
4	3	1	135.4	.11
4	3	1	154.7	.13
4	1	2	0.0	.0
4	1	2	9.7	.023
4	1	2	19.3	.030
4	1	2	38.7	.04
4	1	2	58.0	.047
4	1	2	67.7	.052

4	1	2	77.3	.06
4	1	2	87.0	.063
4	1	2	96.7	.07
4	1	2	106.4	.073
4	1	2	116.0	.08
4	1	2	135.4	.09
4	1	2	154.7	.096
4	1	2	193.4	.11
4	2	2	0.0	.0
4	2	2	9.7	.002
4	2	2	19.3	.005
4	2	2	38.7	.01
4	2	2	58.0	.015
4	2	2	67.7	.018
4	2	2	77.3	.02
4	2	2	87.0	.022
4	2	2	96.7	.025
4	2	2	106.4	.028
4	2	2	116.0	.03
4	2	2	135.4	.04
4	2	2	154.7	.05
4	2	2	193.4	.08
4	3	2	0.0	.0
4	3	2	9.7	.004
4	3	2	19.3	.005
4	3	2	38.7	.008
4	3	2	58.0	.012
4	3	2	67.7	.013
4	3	2	77.3	.015
4	3	2	87.0	.017
4	3	2	96.7	.019
4	3	2	106.4	.021
4	3	2	116.0	.023
4	3	2	135.4	.03
4	3	2	154.7	.04
4	3	2	193.4	.07
4	1	3	0.0	.0
4	1	3	19.3	.006
4	1	3	38.7	.009
4	1	3	58.0	.01
4	1	3	77.3	.013
4	1	3	96.7	.015
4	1	3	116.0	.019
4	1	3	135.4	.022
4	1	3	154.7	.026
4	1	3	193.4	.03
4	2	3	0.0	.0
4	2	3	19.3	.003
4	2	3	38.7	.004
4	2	3	58.0	.005

4	2	3	77.3	.007
4	2	3	96.7	.008
4	2	3	116.0	.01
4	2	3	135.4	.011
4	2	3	154.7	.016
4	2	3	193.4	.017
4	3	3	0.0	.0
4	3	3	19.3	.003
4	3	3	38.7	.005
4	3	3	58.0	.006
4	3	3	77.3	.008
4	3	3	96.7	.009
4	3	3	116.0	.01
4	3	3	135.4	.01
4	3	3	154.7	.015
4	3	3	193.4	.02
4	1	4	0.0	.0
4	1	4	38.7	.003
4	1	4	77.3	.005
4	1	4	116.0	.007
4	1	4	154.7	.01
4	1	4	193.4	.014
4	2	4	0.0	.0
4	2	4	38.7	.008
4	2	4	77.3	.014
4	2	4	116.0	.02
4	2	4	154.7	.026
4	2	4	193.4	.033
4	3	4	0.0	.0
4	3	4	38.7	.002
4	3	4	77.3	.004
4	3	4	116.0	.006
4	3	4	154.7	.009
4	3	4	193.4	.013